POLITECNICO DI MILANO (BOVISA CAMPUS)

School of Industrial and Information Engineering

Master of Science in Mechanical Engineering

MECHANICAL CHARACTERIZATION OF 2D METALLIC SHEETS WITH VOID PATTERN

Supervisor: Prof. MARIO GUAGLIANO

Co-Supervisor: Dr. SARA BAGHERIFARD

Dr. STEFANO MONTI

Graduation Thesis:

THATI JALAPATHY HEMANTH KUMAR

Matr. 873960

Academic Year 2018-2019

ACKNOWLEDGMENT

Firstly, I would like to thank Prof. Mario Guagliano, Department of Mechanical Engineering in giving me the opportunity to work on this thesis. He was always there to answer my queries and guiding me in the right direction. Without his guidance, this thesis would have been impossible. I also thank Dr. Sara Bagherifard and Dr. Stefano Monti, in providing expert support in the modeling and analysis of 2D void patterns using Periodic Boundary Conditions. Whenever I faced problems in the finite element simulations, they would give a proper direction towards a solution which immensely helped me in moving forward. They were always there to supply me with their ideas, which helped me in organizing my work to write a thesis. I would also like to thank my friends and colleagues at Politecnico di Milano for their encouragement and moral support which made my stay in Italy more enjoyable. Finally, I thank my parents who trusted and supported me throughout my studies here in Politecnico di Milano.

TABLE OF CONTENTS

LIST OF FIGURES

LIST OF GRAPHS

LIST OF TABLES

SOMMARIO

Nella fase progettuale di un componente meccanico è molto importante tenere in considerazione le condizioni in cui esso andrà ad operare, nonché lo stato di sforzo che si genera all'interno del componente stesso. Le lastre metalliche forate sono molto utilizzate in ambito industriale, nelle più disparate applicazioni, grazie alla loro "semplicità" di realizzazione. Sono esempi applicazioni per la dissipazione del calore, come filtri o rivestimenti. Anche se le discontinuità geometriche inducono importanti concentrazioni di sforzo all'interno dei componenti meccanici, la realizzazione di specifici pattern è in grado di migliorare o generare interessanti proprietà meccaniche, quali ad esempio la trasformazione di una semplice lastra metallica in struttura auxetica. A questo proposito, il presente studio è volto all'analisi delle proprietà meccaniche ottenute tramite l'applicazione di specifici pattern, aventi ognuno avente il foro con una specifica forma. Per far questo sono state effettuate una serie di analisi numeriche, analizzando una regione rappresentetiva del pattern e applicando la periodicità delle Condizioni al contorno. In totale sono stati analizzate sei diverse forme , tra le quali la Doppia T e la Clessidra hanno dimostrato di poter garantire interessanti proprietà auxetiche, senza introdurre eccessivi fenomeni di concentrazione di sforzo. Queste due forme possono essere utilizzate in sostituzione del più classico foro circolare, nelle più differenti applicazioni pratiche.

ABSTRACT

The stress field in a mechanical component is generally an important phenomenon to consider during the design stage. Perforated metallic sheets are widely used in industry, in many different applications like film cooling, heat dissipation, filtering and many other, mainly thanks to their simple and mass production process. Even though geometrical discontinuity is known to induce stress concentration effects within the mechanical component, the perforated pattern is able to provide interesting structural properties, like auxetic behavior. For this reason, by this study, we investigated the mechanical performance of different void shapes through a series of numerical simulations, by defining a representative element for the pattern and applying Periodic Boundary Conditions to the model. We have simulated six different hole shapes. Among them, the Double T and Hourglass shapes have the ability to introduce auxetic property without introducing important stress concentration effects. These two shapes can be replaced by the traditional pore shapes like circle, ellipse, and rectangles to reduce the stresses in the perforated metal sheets and use the auxetic property for smart applications.

1. INTRODUCTION

Perforated sheets play a major role in various engineering applications for heat transfer, filtering, fencing, sunshades, etc. As this study majorly focuses on metal-related perforated sheets some of the applications can be classified as per the hierarchy Figure 1.1.

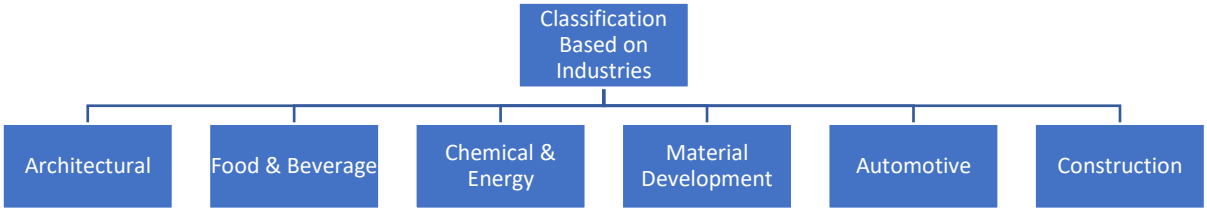

Figure 1.1 Hierarchy of Industries Using Metal Perforated sheets for Various Applications

Based on these industrial classifications mainly two parameters change according to application those are Shape of the perforation and the physical quantities like temperature and load applied. But to focus our study we have considered only load based applications, some examples are Grain dryers and sorters are affected by continues vibration and cyclic loads used in food & beverage industries, similarly, engine and radiator cover used in automobiles are influenced by various loads and temperatures as well. So, when perforated metal sheets undergo force or vibration, they are affected by the stress concentration factor which is dependent on the shape of the pattern. The most common shape widely considered is the circular shape and the circumference of the circle attracts the stresses based on the direction of loading. In the case of shapes which has edges can be the critical points of failure which are independent of the direction of loading. Hence this study has been performed to replace the common shapes with new shapes which could provide some interesting mechanical properties, without interfering with the stress field of the perforated sheets with better stress distribution and load-bearing capacity.

Considering 2D elements to observe stress field and simplify analysis time we have categorized the new shapes in design conditions, with the influence of Size, Profile, Arrangement, Rotation, Width and Porosity which influence the stresses and Poisson's Ratio (section 4.2). Innovation has been also added to this analysis by considering auxetic properties in metal sheets with intricate patterns. Auxetic properties are manly validated based on the Poisson's Ratio of the material when the load is applied. For easier understanding, we have selected six different hole shapes which have supported us to validate our result with evident values of stresses and Poisson's Ratio which will be explained in detail further. Hence using finite element analysis and advanced mechanical design technique we have concluded numerically that we can

increase the durability and reduce faster failure in static load cases by distributing the stresses using Double T and Hourglass shapes (similar to reference [1]).

2. STATE OF THE ART

The vision to explore this study was the behavior of the 2D structures under static loading conditions to improve its stress field distribution and performance indices. The idea was supported by some references which helped us to define boundary conditions and guidelines to design new patterns. “Farhad Javid’s et al.” [1] describes the application were metallic perforated sheets are used as combustion liners, ducts, casings and sealing surfaces for cooling holes of the passage of cold air to the turbine blades. Gas turbines are used from driving tanks, jets, helicopters to power generation and industrial power users in a variety of power needs. They operate at temperatures that exceed the materials ' melting points, so it is necessary to install the system's cooling functionality. Film cooling is an efficient method for reducing the temperatures of the components and is currently used in many aircraft turbines and many turbine engines generating power. Due to the stress caused by temperature variations, these cooling holes are highly prone to fatigue failure. Several studies considered optimizing the shape of the cooling holes, but most of them focused on the functionality of cooling. Typically circular holes were the cooling holes used in these types of structures. But the use of circular holes had limitations on the edges of the holes with increased stress concentration factors, leading to the failure of cooling holes prior to 100k cycles. They replaced circular holes with S-shaped holes in their study and analyzed the results. There was a remarkable change in the deformation mechanism and how crack propagates in the case of S-shaped holes. They have determined from their analysis that the S shapes experience the low-stress value since the mechanism of deformation is found to induce domain rotation between neighboring holes. Thus, the cracks initiated at the concentrations of stress along the s-shaped pores are trapped in low-stress regions and propagated at a much lower rate.

They have conducted an experiment using stainless-steel dog-bone samples which were fabricated out of 1 mm thick stainless-steel sheets characterized by $E = 193$ GPa and $\nu = 0.33$. A square array of 5 X 5 holes with a center-to-center spacing of 10 mm was embedded in their gage section by laser-cutting. Details of the geometry of the sample can be found in Figure 2.1. The circular holes have radius $R = 0.63$ mm, while the S-shaped pores have a length of 6.6 mm and a width of 2 mm (see zoom-in in Fig. 2.1 for the details of S-shaped pores). Importantly, both samples are characterized by the same porosity in the gage section, $\psi = 0.05$.

According to the reference [1], tests were conducted under strain-controlled conditions using a trapezoidal waveform with a frequency of 0.25 Hz. For the planar samples, they used $\epsilon_{max\ applied}$= 0.002 and $\epsilon_{min\ applied}$ = 0, while for the cylindrical samples we used $\epsilon_{max\ applied}$ = 0.004 and $\epsilon_{min\ applied}$ = 0. The specimen failure was defined at the point when a 90% drop in the maximum load (compared to the first cycle) was recorded.

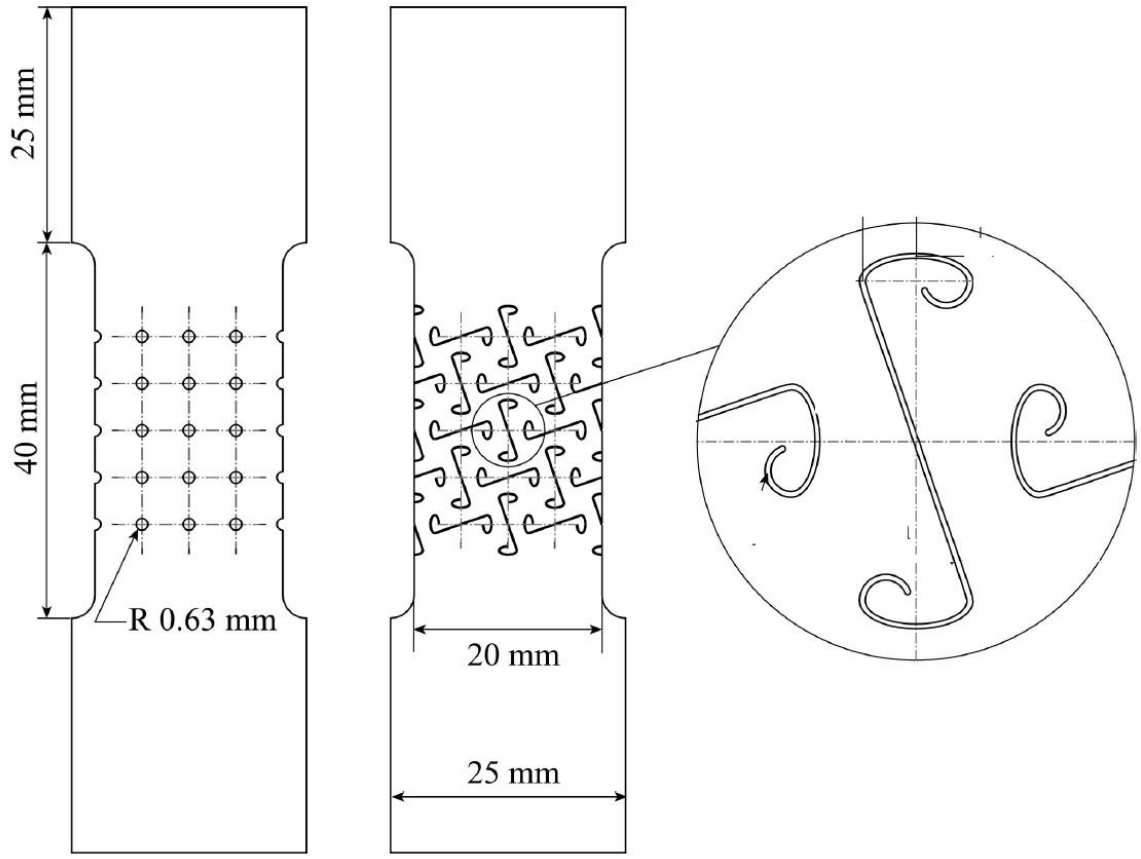

Figure 2.1 Detailed Dimensions of Dog Bone Samples with Circular and S patterns

For a further deeper understanding of different shapes, we have been assisted by "L. Francesconi et al." Reference [2] which presents an assessment of static and dynamic mechanical behavior of low porosity, ductile auxetic metamaterials. Using speckle interferometry and digital image correlation, they used full in-plane displacement fields and the own modes of different geometric structures to investigate and compare with finite element simulations. The results show strong agreement, validation of the theoretical approach used and the establishment of a method for testing and quantitative evaluation of the performance of negative Poisson ratio structures and metamaterials for various purposes and fields in general. According to the author, their findings from this study also increase the knowledge of elastic instability in metallic auxetic structures, with further applications in several engineering fields that can benefit from combining ductile material qualities with additional characteristics typical of these smart structures.

2.1. AUXETIC PROPERTY

According to "Joseph N. Grima and Ruben Gatt" [10] Poisson's Ratio defines the ratio between the transverse strain and axial strain in a loaded material. The extent of deformation a material undergoes when it is uniaxially stretched or compressed are quantified through Poisson's Ratio. For most of the conventional materials, the value of Poisson's Ratio is positive. But the Poisson's Ratio not necessarily to be always positive. The classical theory of elasticity suggests that the Poisson's Ratio of isotropic materials can have the values within -1 to 0.5. and the range is wider for orthotropic and anisotropic materials. Negative Poisson's Ratios have been discovered for naturally occurring or man-made metals including foams, polymers, cubic lattice, naturally layered ceramics, ferroelectric polycrystalline ceramics, metals, zeolites, etc. Various model structures and mechanisms which exhibit negative Poisson's Ratio include re-entrant units, rotating rigid units described in Figure 2.2. The materials which exhibit negative Poisson's Ratio are auxetic materials. The auxetic materials exhibit the very unusual property of becoming wider when stretched and narrower when compressed.

Figure 2.2 Shows the arrangement of shapes leading to Negative Poisson's ratio

Based on Reference [10] Auxetic materials are of interest due to their counterintuitive behavior under deformation and enhanced properties. It has been found that auxeticity can be described in terms of the geometry of the material system and deformation mechanism when loaded. The negative Poisson's Ratio is a scale-independent property i.e the auxetic behavior could be achieved at a macroscopic or microscopic level, or even at the mesoscopic and molecular level. These materials demonstrate unique and enhanced mechanical properties compared to conventional materials. It has been shown experimentally that the indentation resistance of auxetic materials has been enhanced up to four times when compared with their conventional equivalent. Other enhanced properties are mechanical hardness, fracture toughness, and stiffness based on Reference [14]. In terms of the dynamic performance, auxetic materials also show an overall superiority regarding damping and acoustic properties compared to the conventional materials. Owing to their easy availability, and desirable mechanical properties,

auxetic materials find a broad range of applications in many industrial sectors, especially in automotive, aerospace, and marine industries. More and more auxetic materials and structures with different microstructures are used to replace conventional counterparts and have achieved satisfactory results.

Today, a variety of auxetic materials and structures have been discovered, fabricated or synthesized ranging from the macroscopic down to the molecular levels. The design of 2D systems capable of retaining a negative Poisson's Ratio at low values of porosity remains a challenge. Geometrical optimization of 2D structures could lead to the exhibition of auxetic properties which is also included in the current study. The combination of various geometry optimization leads to an increase in negative Poisson's Ratio. With some combinations, we have also obtained Poisson's Ratio values which are close to 0. This is also an enhanced property of the system that these systems neither get wider nor thinner when stretched or compressed. Some applications of auxetic properties which are implemented on high-porosity foam structures have been recently introduced, including actuators, sensors, self tunable photonic and phononic crystals, smart objects and surfaces, protection devices, enhanced shock-absorption devices, self-cleaning filters, and strain amplifiers, etc. We have analyzed our study based on the simulation results of the reference, For the sake of simplification and clarity they have named their patterns as circle (Fig. 2.2(a)), stop hole (Fig. 2.2(b)), ellipse (Fig. 2.2(c)) and double-T (Fig. 2.2(d)) were assigned to the four samples referencing the geometry of the pores, but neither parametric studies nor optimization analyses have been performed by the author to address the shapes selection, minimize the stress concentration, or enhance the in-plane stiffness and the buckling strength. The rectangular samples (Fig. 2.2) are of dimension 300 mm × 50 mm ×1 mm made of stainless steel were cut using a wire electrical discharge machine (EDM) and a computer numerical control (CNC) machine. They used these samples for Tensile static tests to compare between Digital Image correlation, speckle interferometry, and Finite element analysis.

Based on Reference [2] the base cells (shown in the four magnified boxes on the right side of Fig. 2.3) of each sample follow a square array; the geometrical center of each void is placed 6.25 mm away from the next one both in the horizontal and in the vertical direction. The four samples can all be considered low porosity structures, because they exhibit a level of porosity (i.e., the total volume of the voids divided by the total volume of the material), of about 4.55%. These structures are analyzed and validated in section 3.1.1 for learning the auxetic property of perforated metallic sheets with different void shapes.

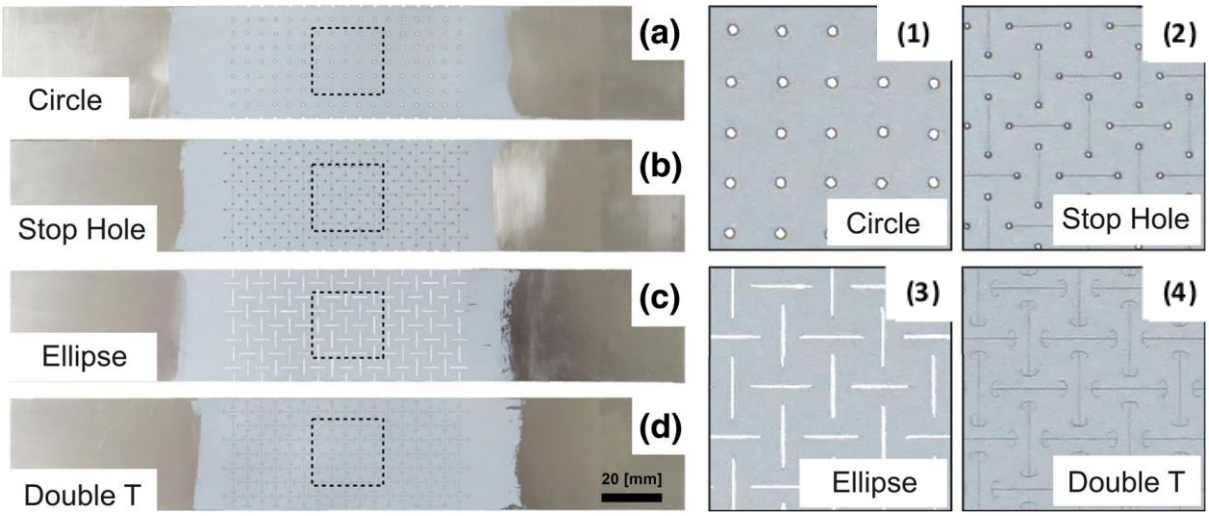

Figure 2.3 Fabricated samples for testing (a) Circle(b) Stop Hole(c)Ellipse(d) Double T

The main parameter the author has considered for the comparison of shapes is the displacement in horizontal and vertical directions which will be the used to determine the conclusion for best auxetic behavior of the patterns which are considered. All tests were performed well within the sample elastic limit to avoid local plasticization at feature tips; the constitutive stress-strain relationship is considered linear for all presented investigations. The three samples were loaded along the longitudinal direction with a maximum displacement of 0.1 mm From a macroscopic point of view they look similar, but some important differences are apparent: the displacements in the direction orthogonal to the load (U1) differ largely because they are a function of the stiffness of the samples and, hence, of the features' shape and of the tessellation chosen. The largest U1 displacements were predictably obtained from the most compliant sample (the double-T, Fig. 2.3)

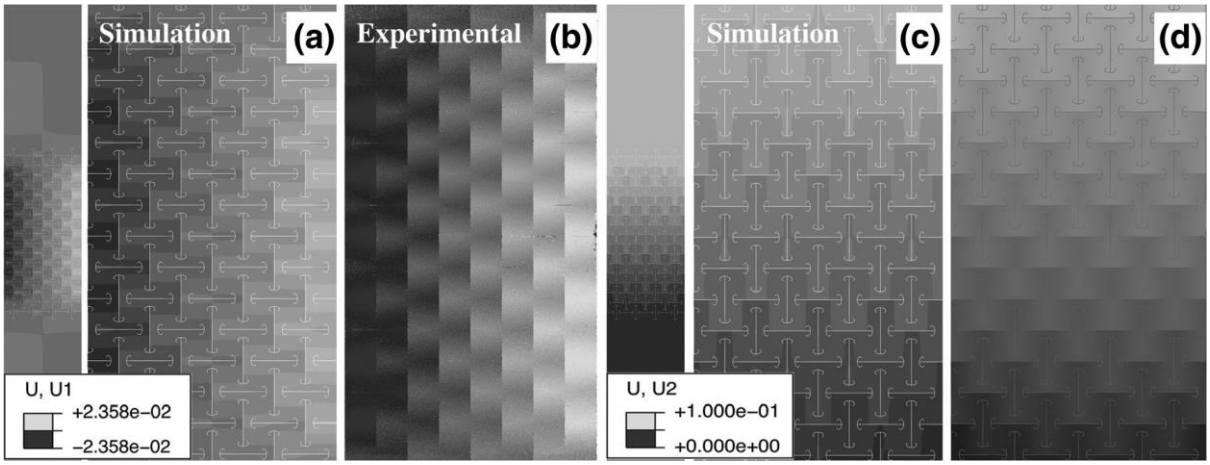

Figure 2.4 Horizontal (a and b) and Vertical (c and d) displacements (reported in millimeters) of the double-T sample under a static tensile load

According to the Reference [2] the differences in the magnitude of the U1 displacements, the three auxetic samples behave, an expansion at the midsection can be detected due to the application of a tensile load. It is possible to track the evolution of the Horizontal displacement in the central section of the sample; the Experimental displacement maps highlight the jumps in the displacement fields due to the interruption of the material continuity caused by the presence of the double-T shaped cut. These discontinuities allow the base cells to rotate about the ligaments of material that connects them and finally drive the motion of the surface point, leading to an auxetic expansion. The estimation of Poisson's Ratio by the author is by sampling displacement at 8 points along each of the four boundaries of the central regions. Each set of 8 points are averaged (arithmetic mean) to compute the average displacements at the boundaries: $(u_x)^L$, $(u_x)^R$, $(u_y)^T$, $(u_y)^B$.

$$(\epsilon_{xx}) = \frac{(u_x)^R - (u_x)^L}{L_0} \; ; (\epsilon_{yy}) = \frac{(u_x)^R - (u_x)^L}{L_0}$$

where L0 is denoting the distance between the top/ bottom and left/ right boundaries in the undeformed configuration. The local strain averages are then used to calculate an effective Poisson's Ratio

$$\nu = \frac{-(\epsilon_{xx})}{(\epsilon_{yy})}$$

For designing insights Reference [3] helped us to understand that the Poisson's Ratio can be effectively controlled by changing the aspect ratio of voids. The structure is characterized by positive values of the Poisson ratio for low aspect ratios. However, as the aspect ratio increases the Poisson ratio's value monotonically decreases and becomes negative. Based on this condition they have kept porosity similar and changed the aspect ratio to analyze the behavior of the shapes. They have considered circle and ellipse shape to observe the auxetic behavior using U1 & U2 displacements through which Poisson ratio can give the result. The author describes the aspect ratio in a/b ratio which implies circle has a/b ratio as 1 and the deigned ellipse had a/b~30 (above 30 the ellipse will become very pointy which will induce more stresses). So, like References [1],[2] they have also performed the static tensile test and compared with the simulation results. The results confirm that the void aspect ratio can be used effectively to design low porosity structures and Poisson's Ratio's negative value. The high aspect ratio ellipses result in the material characterized by a significant negative value of Poisson's Ratio. For the circular shape, the ratio of the Poisson is still close to the ratio of the bulk modulus Poisson, but for the ellipse, it is completely different where the value for an infinite structure has approached -0.65. In Figure 2.4 they have displacements of U1 and U2 for the circular and ellipse shape in their respective aspect ratio.

With Figure 2.4 it is clearly evident new shapes can be designed for the same applications which can better load bearing capabilities and enhanced auxetic behavior compared to current shapes which have a lower fatigue life. Using the approach of References described above and mentioned in references section we have developed a numerical analysis which helps us to analyze the stress distribution, shape behavior under loading when periodic boundary conditions are applied, auxetic behavior and fatigue life of perforated metal sheets.

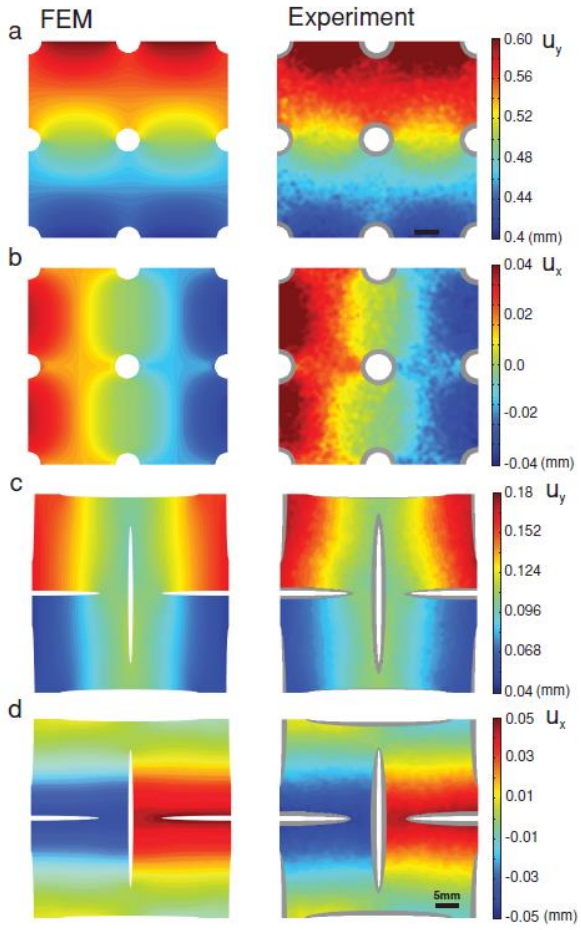

Figure 2.5 U1 & U2 Displacement plots for circle and ellipse shape

2.2. PERIODIC BOUNDARY CONDITION

Periodic boundary conditions are a set of boundary conditions which are used to simulate an infinite structure by simply modeling a finite representative volume. A finite representative volume is often called a unit cell. In our study, we use PBC to approximate a 10mm X 10mm to infinite structures. In periodic boundary conditions, an infinite lattice system is formed simply by repeating the simulation box throughout space (as shown in Figure 2.5). When a molecule leaves the box, one of its images will enter through the opposite face with exactly the same way and direction. The molecules in the simulation box will conserve and the system can be thought of as having no surface based on Reference [4].

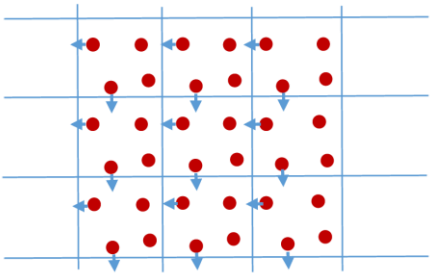

Figure 2.6 A 2-D Periodic Boundary Condition cell

PBC is a great option to reduce computational time and computational cost in case of modeling large structures. Periodic boundary conditions are commonly applied in molecular dynamics, dislocation dynamics and material modeling to eliminate the existence of surface and avoid a huge number of molecules or large size of simulation. We have followed [4] to define PBC equations in our study. Also, we have been some modifications to suit our requirement. A strain controlled PBC may be specified by following equations.

$$u(x+L) = u(x) + \varepsilon^0 x \qquad \forall\, x \in B^2_{\delta} \qquad (1)$$

$$u(x+L) = u(x) \qquad (2)$$

$$t(x+L) = -t(x) \qquad \forall\, x \in B^1_{\delta} \qquad (3)$$

where u is the displacement at x, ε^0 is the strain applied to the RVE, t is the traction force and B^1_{δ} represents the boundary B whose normal is along "1" direction.

- **Constraint Equations**

We apply PBC through linear constraint equation in ABAQUS. Multi-points may be constrained by a general linear combination of nodal variables. The summation of the product of a coefficient and the corresponding nodal variable is equal to zero. We define a general linear homogenous equation

$$A_1 u^P_i + A_2 u^Q_j + \ldots\ldots\ldots\ldots\ldots\ldots + A_N u^R_k = 0 \qquad (4)$$

Where r is a node, k is the degree of freedom and A_N is a constant coefficient that defines the relative motion of nodes.

- **Dummy Node**

To apply PBC using constraint equations described above, one abstract concept of "dummy node" is introduced in Abaqus. We rewrite equation (4) by replacing zero by a non-zero value u.

$$A_1 u^P{}_i + A_2 u^Q{}_j + \ldots\ldots\ldots\ldots\ldots + A_N u^R{}_k = u \qquad (5)$$

- **Definition of equation**

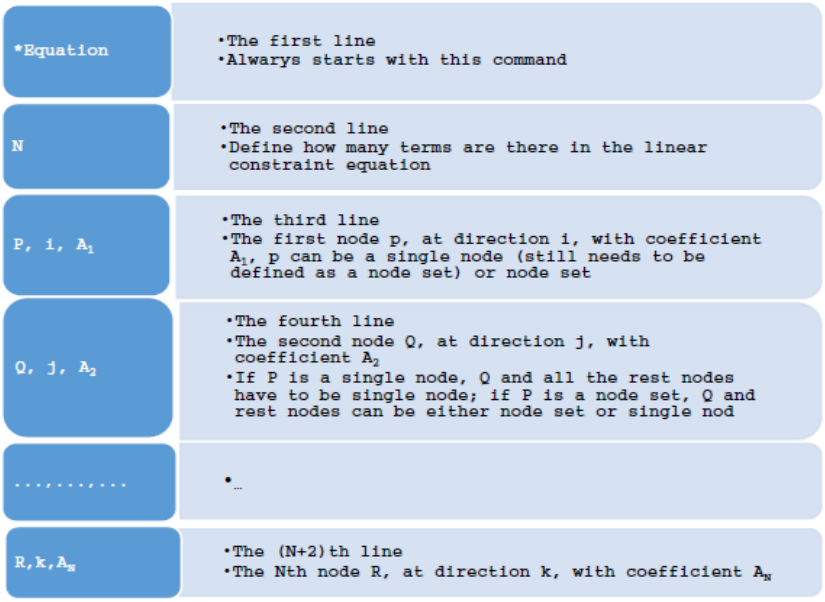

Figure 2.7 Definition of * Equation

```
*Equation
3                    ** equation has 3 terms
Left, 1, 1           ** left surface node set, dof = 1, coeff = 1
Right, 1, -1         ** right surface node set, dof = 1, coeff = -1
*Equation
3                    ** equation has 3 terms
Left, 2, 1           ** left surface node set, dof = 2, coeff = 1
Right, 2, -1         ** right surface node set, dof = 2, coeff = -1
10000, 2, 1          ** dummy node z=10000, dof = 2, coeff = 1
```

RVE description as per our study requirement

$$u_1{}^{left} + u_1{}^{right} = 0 \qquad (6)$$

$$u_2{}^{top} - u_2{}^{bottom} = -0.01 \qquad (7)$$

So, we have embedded these equations in a python script (Appendix A) which will be used to run in Abaqus module to generate Periodic boundary conditions. The algorithm to generate paired nodes for the Circular pattern simulated in Reference [1] is explained below.

2.3. MANUFACTURING TECHNOLOGY

Laser drilling has been considered as the best technology when compared to other high accuracy machining options. A comparison of basic parameters which influence our shape designs is described in Table 2.1.

Table 2.1 Parameter comparison of Laser Drilling, CNC punch and Waterjet

Parameters	**Laser Drilling**	**CNC Punch**	**Waterjet**
Accuracy (mm)	±0.025	±0.25	±0.1
Thickness (mm)	6	8	70
Cutting Speed	2 m / minute	1600 punches/ minute	50mm / Minute
Quality of Edge	Excellent	Fair	Excellent
HAZ	Yes	No	No
Material Distortion	Cuts by melting, resulting in material heat distortion.	Some distortion depends on the thickness	No Distortion
Process Type	Non-Contact	Contact	Non-Contact

With the Table above we can infer that laser drilling is the most accurate manufacturing method currently which will be used to create shapes based on the numerical analyses described in this study. As the applications of these complicated perforations might be the limited speed of cutting can be compromised hence faster process like CNC punching won't be able to create shapes which have intricate dimensions. Similarly, waterjet being a non-contact process it is very difficult to control the flow of water to create smooth curvatures with smaller dimensions. The minimum cut distance considered in our study is 0.1mm and the minimum distance between two elements is considered to be 0.2mm which can be achieved using laser drilling based on References [11-13]. Considering mass production we have described the types of the manufacturing process for perforated metal sheets.

2.3.1. Types of Manufacturing Process for Perforated Metal Sheet.

Based on reference [9] there are 3 main manufacturing processes used to create Perforated Metal sheets.

a) Punch Press

The majority of Perforated Metal sheets is manufactured with a device called a Punching Press. Punch Press machines feature sharp perforation tools that can be customized to desired hole size and shape. There are a couple of types of Punch Presses. Wide Punch Presses feature long rows of punching rams. When sheet metal, whether plate or coil, is passed through this machine, the rams descend upon the material to strike and perforate entire rows of holes in one motion. For this reason, Wide Punch Presses are ideal for punching large amounts of perforations at quick speeds. Another Punch Press is the Sectional XY Axis machine. Sectional XY Axis Punch Presses do not typically have long rows of perforation tools, unlike Wide Punch Presses. Rather, they will feature either a single die or a limited cluster of punching rams. Instead of passing sheet metal through this machine, the die or punching ram clusters are moved across the stationary material section by section. As you can imagine, this method can sometimes be a lengthier process. However, it is optimal for Perforated patterns that are non-repetitive or have complex designs. Typically, with either Punch Press method, a certain amount of material along the length of the sheet will be reserved as unperforated. This is done to create margins or solid blank areas around the edges of the material.

b) Rotary Pinned Perforation Roller

As one of the most efficient methods of perforating metal, Rotary Pinned Perforation is a popular process for standard Perforated sheets. This method begins with large cylinders equipped with sharp, pointed needles along the outside. Sheet metal is then run underneath these structures, and as the cylinders rotate the needles continuously punch the sheet passing below. In some cases, the needles will be heated in order to melt the metal on the inside of the punched holes. This is done to reinforce the rings of the perforations and increase strength. The cylinders can be rotated at considerably fast speeds, so Rotary Pinned Perforation is optimal for punching numerous identical holes at a quick rate.

c) Laser Drilling

Laser Perforation is a process where focused, highly accurate beams burn holes in sheet metal beneath them. Lasers are incredibly precise and versatile methods of perforation but can be costly and time-consuming for large volumes.

3. MODEL VERIFICATION AND DESIGN CONSIDERATIONS

To begin with our own design and analysis it is very crucial to validate our design procedure with similar models or area of interest. We have chosen ABAQUS for our designing and analysis of the patterns and also, the filtering of References for our study was performed based on this criterion. For validation purpose, we have kept the same material properties and boundary conditions to achieve the same result of the Reference referred. With this approach, we can understand the design procedure used by various authors and recreate effective designs out of it. So, we have validated 3 case studies which will be the foundation of our design procedures.

3.1. CASE STUDIES AND VALIDATIONS

Selection of References for modal validation was done based on some ground rules. Firstly they should be metal perforated sheets with respective shapes of their choice. Secondly, the perforated sheets should undergo static tensile loading finite element analysis in ABAQUS which will be easier and genuine for comparison purposes. Finally, the main criterion of our study is applying Periodic Boundary Conditions (Section 2.2) on the model to limit simulation time, so References which use periodic boundary condition will verify our results.

3.1.1. Case 1: Validating low porosity metallic auxetic structures without periodic boundary conditions.

This validation is based on Reference [2] in which the " L. Francesconi et al." is evaluating the auxetic behavior of 4 different shapes (showed in Figure 2.1) namely a) Circle b) Stop Hole c) Ellipse d) Double T. Author has performed experimental and modal analysis also which we won't be considering for our study as it will complicate the scope of designing patterns under static loading only. So, we would replicate the same patterns so as to verify our method and accuracy of the software.

Model Specification

It's a 300 x 50 mm stainless steel AISI 304 plates with a modulus of elasticity 200 GPa having a yield stress of 200 MPa and Poisson's ratio of 0.29. Maintaining same porosity level of 4.55% the 4 patterns namely a) Circle b) Stop Hole c) Ellipse d) Double T is designed in Abaqus for finite element analysis. The author has compared his study with experimental analysis also which we won't be considered as our study is based on numerical conclusion and discovery of new patterns. The main parameter considered by the author for comparison of patterns is the

displacement parameters, as the Finite element analysis is performed in 2D space U1 & U2 will be the judging parameters.

Boundary conditions and Meshing Parameters

All the patterns have the same boundary conditions and meshing parameters for the numerical comparison. 0.1 mm displacement has been given to load the model with static loading based on the reference [2] with Encastering at the bottom and pulling in Vertical direction. The remaining boundaries are considered as traction free. Tetrahedral element shape has been chosen with quadratic tetrahedral CPS6 element type applying plane stress condition.

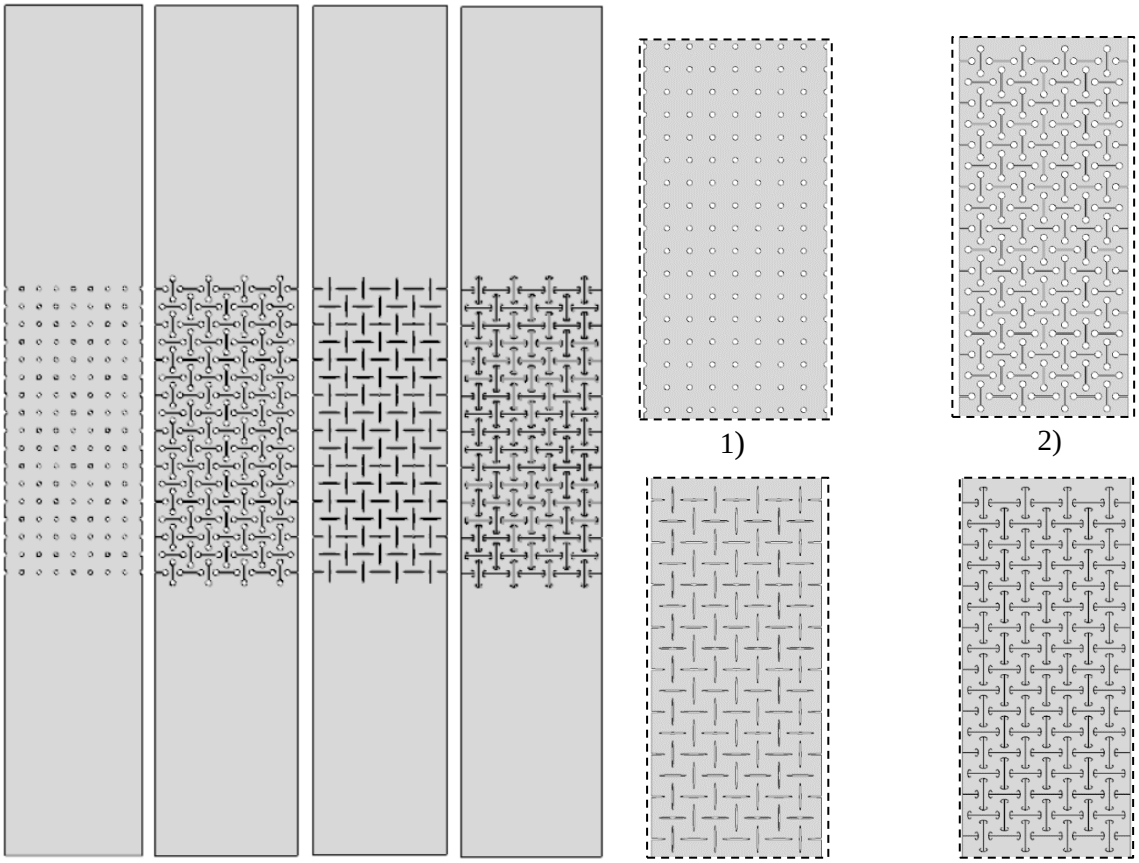

a) Circle b) StopHole c) Ellipse d) Double T

Figure 3.1 Abaqus Part Models with Full-Scaled and Zoomed View designed

a) Circle

According to the author this shape won't exhibit auxetic property due to its Poisson's Ratio values which are always positive under static load, hence he didn't perform any finite element analysis on circular patterns. But for our understanding and comparison purpose, we performed it to verify the author's conclusion. Hence designing 0.75 mm of circular patterns with 6.25 mm center to center distance arrangement we have performed the simulation.

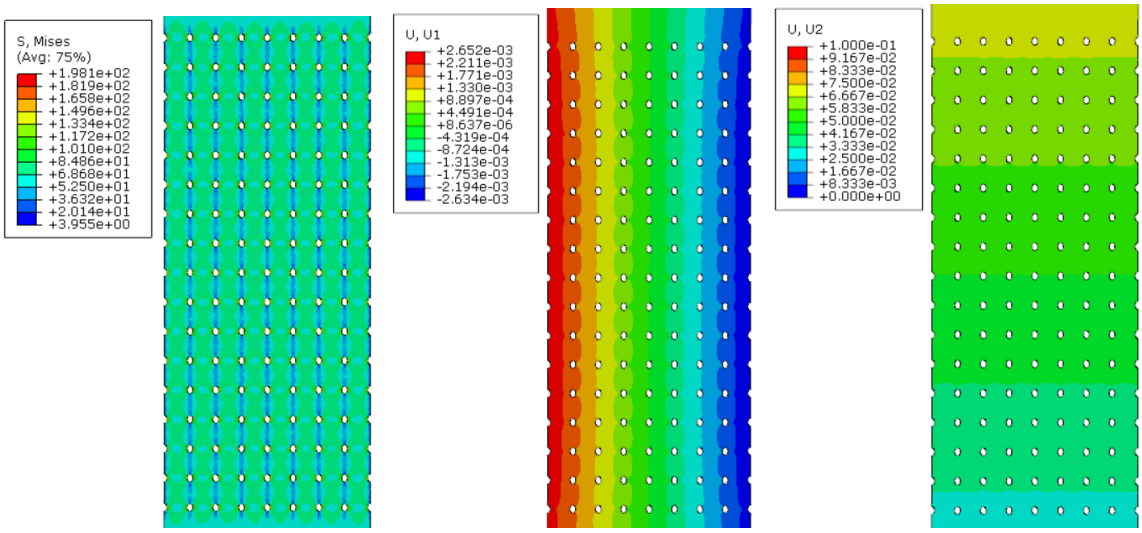

Figure 3.2 Zoomed View of model Stresses, Displacement in X (U1) and Y (U2) directions

The numerical analysis shows visually that the circular patterns are being stretched into an ellipse shape which shrinks the plate inwards hence it's understood that circular patterns cannot exhibit auxetic behavior. According to the simulation results we can see in Figure 3.2 that the maximum Von Mises stress is 198.1 Mpa which will around the circumference of the pattern were the stretching begins and the Critical Area of crack propagation. When understanding displacements Horizontal direction is the most crucial one to observe which is U1. According to the Figure above we have the maximum displacement of the edges of the plate in the Horizontal direction is 0.000265 mm from the center of the plate, which we will use for comparison purposes in the upcoming comparison section. Vertical direction displacement which is U2 is used to just verify the displacement value to induce tensile loading on the plates. According to the author, they won't be considering stresses as their main parameter of control as they are more focused into the auxetic property which means they are more interested into the displacements in the Horizontal direction. But in our study, we also include the reduction of Von Mises stresses also we would be comparing the stress values in the upcoming results. Even if the circular shape doesn’t exhibit auxetic property they are the most widely used shape to create perforated metallic sheets in various applications. As they are easy to mass produce with precise accuracy using any type of mass production processes in which some of them are CNC punching, nibbling process, laser drilling, etc. But they have fast crack propagation issues when a crack has been initiated which can create multiple failures in the whole metal sheet according to Reference [1]. Hence, upcoming shapes can possibly avoid these issues and better stress field distribution.

b) Stop Hole

As the name suggested by the author in Reference [2] this pattern has two holes at the ends and a strip in between. In Reference [2] they have simulated in Abaqus with the conditions mentioned above to observe this pattern auxetic behavior. Hence, we would be able to compare our results with the Reference [2] to authenticate our simulation and extract positives to design our shapes.

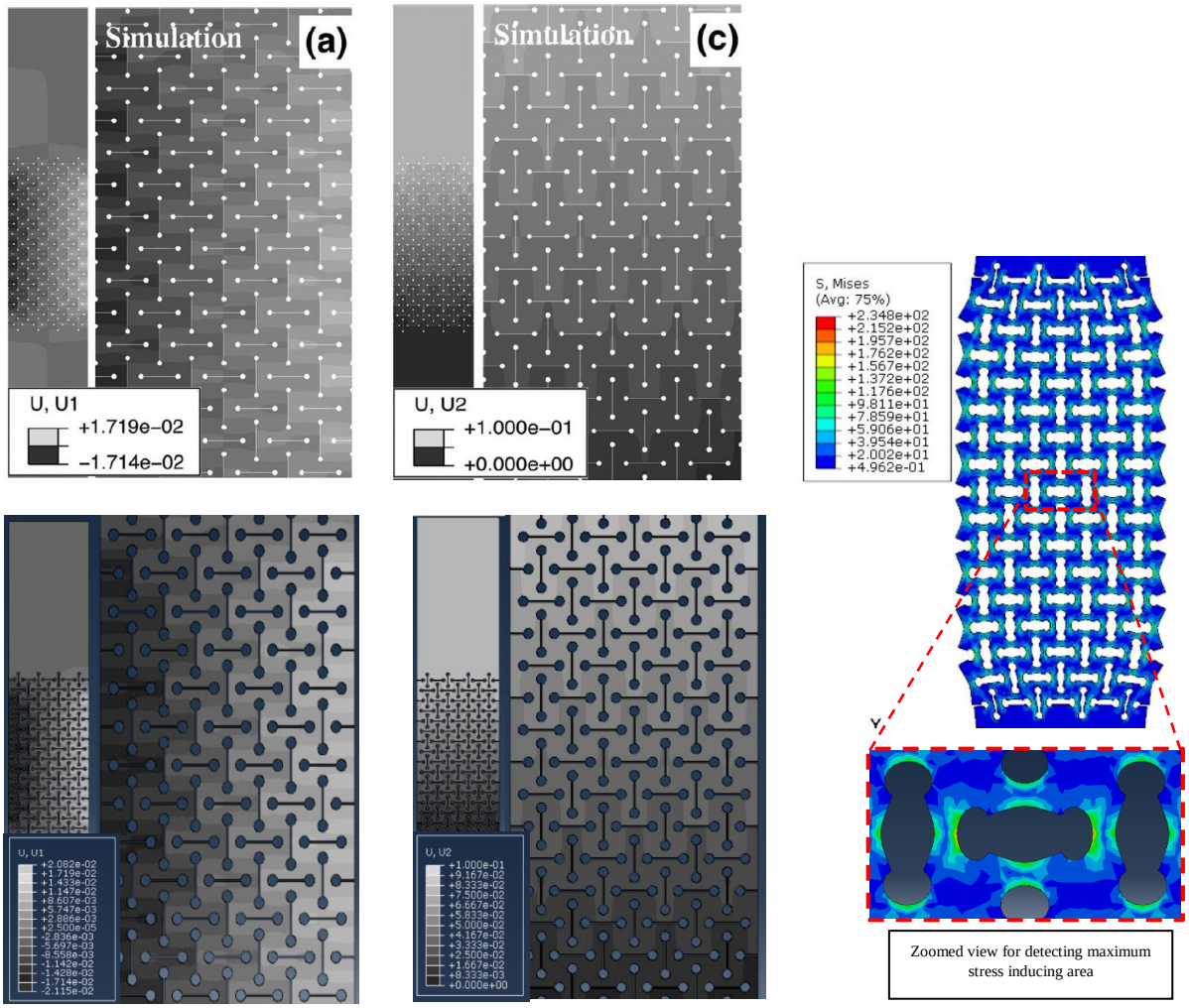

Figure 3.3 Displacement Comparison in U1 &U2 direction of Stop Hole pattern with Reference (Top) and Validation (Bottom) with Von Mises Plot (Right)

With comparison, we have achieved almost the same result as an author with 3.63% error which is due to meshing parameter differences as the author didn't mention about meshing parameters in the reference. According to Reference [2], they have a maximum displacement of Stop Hole pattern 0.00171 mm in the Horizontal direction and 0.1 mm in the Vertical direction which is the loading direction. Trying to recreate the same values we achieved maximum displacement of 0.00208 mm in the Horizontal direction and 0.1 mm in the Vertical direction with 234.8 MPa Von Mises stress. With these results, the author is evident that stop hole shape exhibits

auxetic behavior as there is 544% (% increase between 0.00171 and 0.000265 mm) increase of displacement value in the Horizontal direction when compared to the circular pattern plate (0.000265 mm) shown in Figure 3.2. But when we compare the maximum Von Mises stresses of the stop hole pattern in Figure 3.3 with the circular shape in Figure 3.2 there is an increase of 36.1 MPa in the stop hole plate. Which infers that even if stop hole pattern exhibit auxetic behavior it induces more stresses into the plate. The maximum stress generation (red and green regions) is occurring in the area were the stop hole is most stretched which is at the tips of the top and bottom circles and in the middle of the strip region as shown in Figure 3.3 zoomed Von Mises stress distributions performed in Abaqus.

c) Ellipse

Ellipse is formed when the aspect ratio of the circle is changed as stated in Reference [2]. So, the author infers that we can achieve auxetic behavior if we tune the aspect ratio of a regular ellipse (the ratio between the two major axes). Unfortunately, if we increase the aspect ratio really high, we can form really sharp tips in the ellipse which will increase the stress concentration factor leading to plasticity and fracture based on Reference [2].

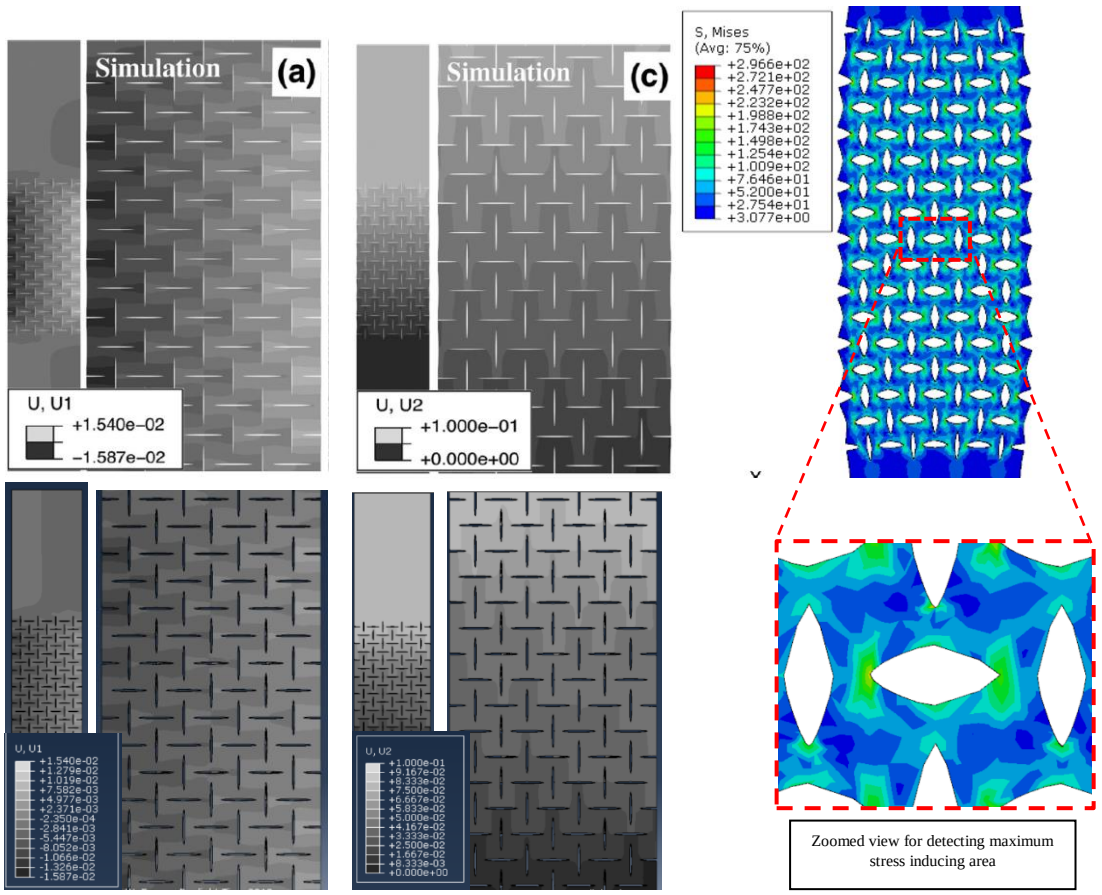

Figure 3.4 Displacement Comparison in U1 &U2 direction of Ellipse pattern with Reference (Top) and Validation (Bottom) with Von Mises Plot (Right)

So, we have recreated the ellipse shape in Figure 3.4 with the same aspect ratio of the Reference [2] and this time we have acquired the same result as obtained by the author. The Horizontal direction maximum displacement of the ellipse plate as shown in Figure 3.4 is 0.00154 mm and 0.1 mm is unchanged in the Vertical direction. Similarly as stated above when compared to the circular shape (0.000265 mm) there is an increase of 481% (% increase between 0.00154 and 0.000265 mm) of displacement value in the Horizontal direction which indicates auxetic behavior. Considering maximum Von Mises stress the results exhibit in Figure 3.4 is 296.6 MPa which is 98.5 MPa more when compared to a circular shape in Figure 3.2. This is due to the sharp edges of the ellipse (shown in Figure 3.4) inducing more stresses (red and green region) in the plate.

d) Double T

Based on the authors in Reference [2] justification they have designed this shape with the motive to reduce Von Mises stresses in the ellipse shape described in Figure 3.4. As the name indicates it has two semi-circular inscriptions at the top and bottom edges which visually looks like a 'T' alphabet and a strip in between to complete the patterns (shown in Figure 3.5).

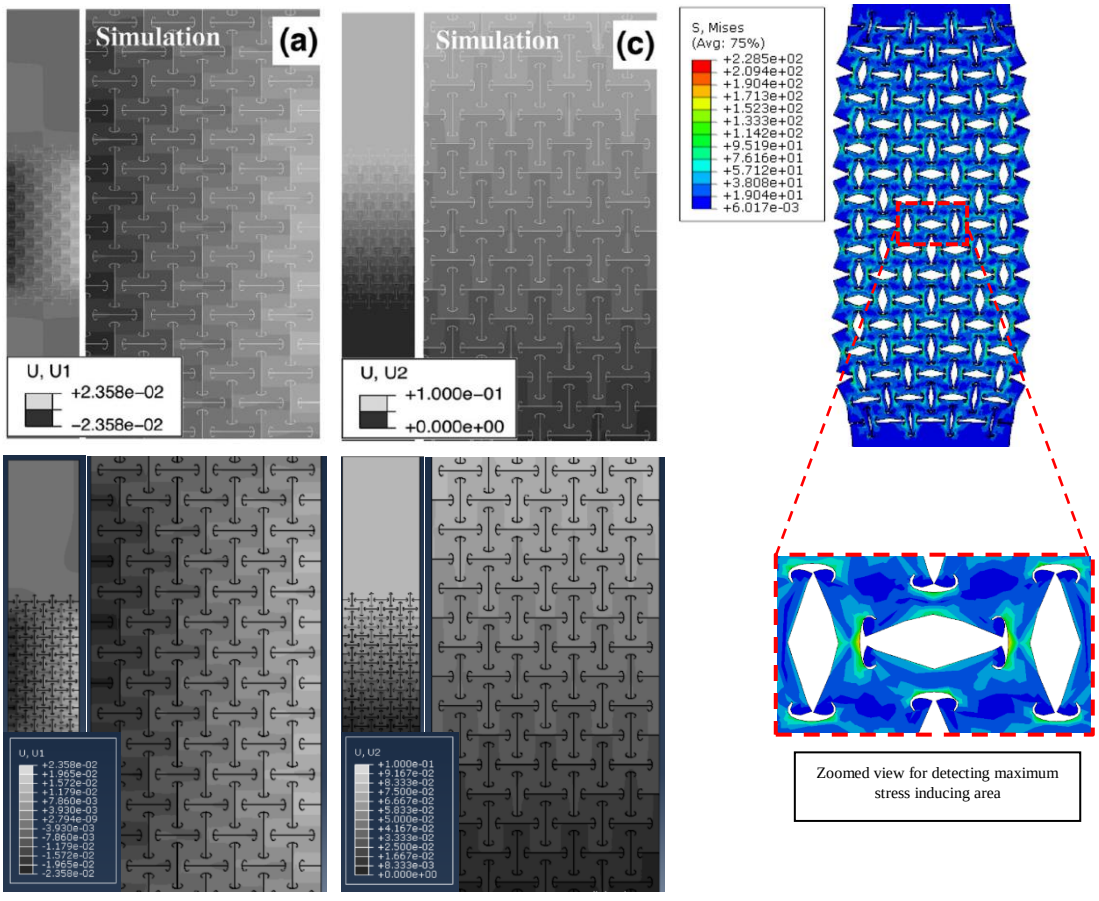

Figure 3.5 Displacement Comparison in U1 &U2 direction of Double T pattern with Reference (Top) and Validation (Bottom) with Von Mises Plot (Right)

We were able to completely recreate the same maximum displacement value generated by in Reference [2] for Double T shape with no error. Upon validation Horizontal direction maximum displacement is 0.00235 mm (shown in Figure 3.5) which is 786% (% increase between 0.00235 and 0.000265 mm) more when compared to the circular pattern (0.000265 mm) in Figure 2.2, hence Double T shape also exhibit the best auxetic behavior. The Vertical direction maximum displacement is 0.1 mm which is unchanged due to the loading direction. We have obtained Maximum Von Mises stresses of 228.5 MPa according to the simulation result in Figure 2.5. There is an increase of 30.4 MPa Maximum Von Mises stresses in case of Double T pattern, which is due to the maximum stretched area (red and green regions) that is at the tips of the top and bottom edges as observed in stress plots in Figure 3.5.

Comparison of Displacements and Von Mises Stresses

This section summarises the discussion above where we can establish the best pattern exhibiting auxetic behavior of the 4 shapes described in section 3.1.1 and authenticated by the Reference [2].

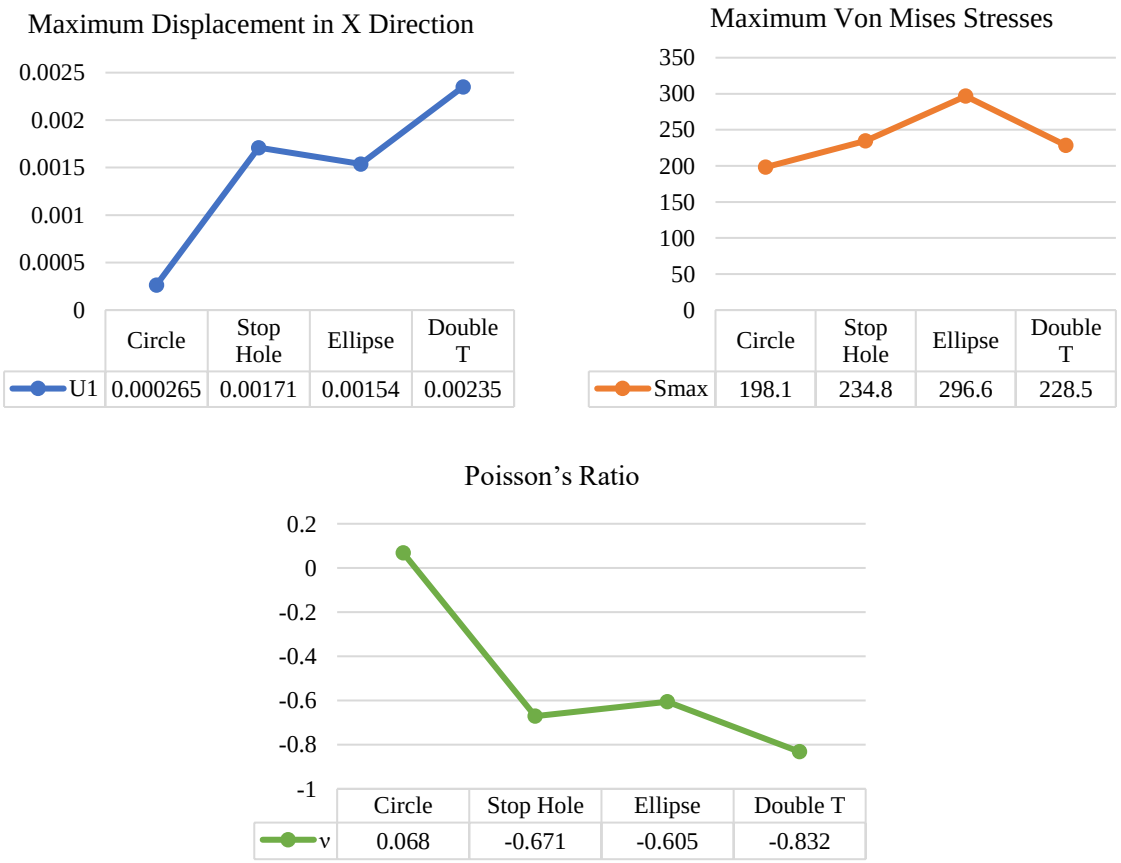

Graph 3.1 Plots describing Displacements, Maximum Von Mises stresses and Poisson's Ratio of 4 different patterns

When we observe in graph 3.1(plotted based on Reference[2] data) the maximum displacement in the Horizontal direction is achieved by the Double T shape and which can be verified by the Poisson's Ratio value of -0.832 when compared to other values obtained by other shapes. According to author even considering differences in the magnitude of the U1 displacements, the three auxetic samples namely Stop Hole, Ellipse and Double T have similar behavior (Figs. 3.3, 3.4 and 3.5) expansion at the mid-section can be detected by applying a tensile load. The evolution of the Horizontal displacement in the central section of the sample can be tracked; the experimental displacement maps highlight the jumps in the displacement fields because of the interruption of the continuity of the material caused by the presence of the double-T-shaped cut. These discontinuities enable the base cells to rotate about the material ligaments that connect them and ultimately drive the surface point movement, resulting in an auxetic expansion. This effect can be observed in Double T (Fig 3.5) and for the stope hole (Fig 3.3) plates, while it is lesser in ellipse shape due to its lower displacements in the Horizontal direction. The displacement maps also show that the mechanical response of the base cells of the samples is highly non - homogeneous, a factor of some importance in the design of this class of structures. It is also evident that the global displacement of the sample in the orthogonal direction of the load applicable is produced by the joint participation of all the base cells and fostered by the discontinuity formed by the presence and shape of the features. In Figures 3.4 and 3.5 the contour plots with accentuated gray level scales indicate step changes in the displacement gradient in the vicinity of the characteristics and a severe increase/concentration of the surface movement around the cuts. Even if the Double T pattern has higher Von Mises stress of 30.4 MPa when compared to circular shape according to graph 3.1 which can be generated locally in very small areas and can be a trade-off for introducing auxetic properties to the material according to the Reference [2].

3.1.2. Case 2: Validating the design of porous structures with enhanced fatigue life.

This case study is based on Reference [1] written by "Farhad Javid et al." were they have addressed with the issue of fatigue failure of perforated sheets with circular patterns due to stresses induced due to temperature variations during operations. They have demonstrated both experimentally and numerically that the fatigue life of the perforated sheets with circular patterns can be greatly enhanced by replacing with S-shaped patterns in the metal sheets. They have mentioned that life of metallic sheet with a square array of conventional circular holes is <100k cycles, which can be increased up to a million cycles when replaced by these S-shaped patterns. To reach these results the author has performed numerical analysis in Abaqus to compare Von Mises stresses of both shapes using Periodic Boundary Conditions described in

section 2.2. Also, the author has evaluated the normalized stresses by changing the aspect ratio of the circle in four different values which gives a better insight into stress distribution in the plate while maintaining the same porosity. Moreover, they have also performed crack propagation study and experimental analysis which we won't be considering for our validation because these will complicate our objective to design and optimize new shapes.

3.1.2.1. The algorithm to generate paired nodes in a 10 x 10 mm plate.

As our numerical analysis is mostly based on a 10 x 10 mm plate, we are going to explain the procedure to run our python script (Appendix A) using the model in Reference [1].

1. To run the python script we need to initially generate the script file of Abaqus which contains the Model with constrained dimensions, applied material properties and appropriate Meshing with required element type then save the model to generate the Abaqus jnl file.

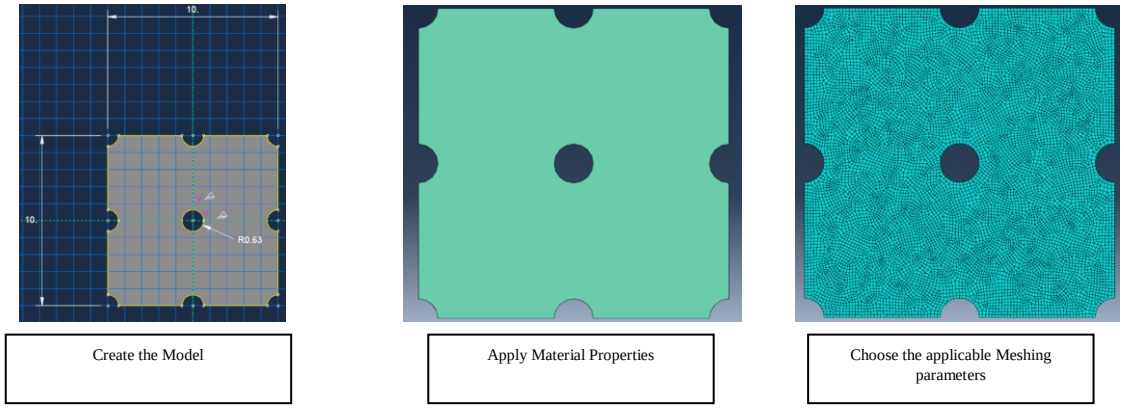

Figure 3.6 Procedure to generate Abaqus script with Model and Meshing parameters

2. Once the .jnl file is generated we can change the extension to .py to convert it to python script for inserting our codes in Appendix A.1. At the beginning of the script, we have inserted an execution command (execfile ('AbaqusScriptFunc.py')) which will run function script available in the same folder.
3. The logic of 'AbaqusScriptFuc.py' (Appendix A.2) is it creates two reference points at the origin which is basically used to connect Top and Bottom nodes with reference point 1 and Left and Right nodes with reference point 2. Then an 'if' loop is initiated which checks the distance between nodes to ensure they are inside the dimensions and then Periodic Boundary Conditions related equations mentioned in section 2.2 are applied till every node is constrained.

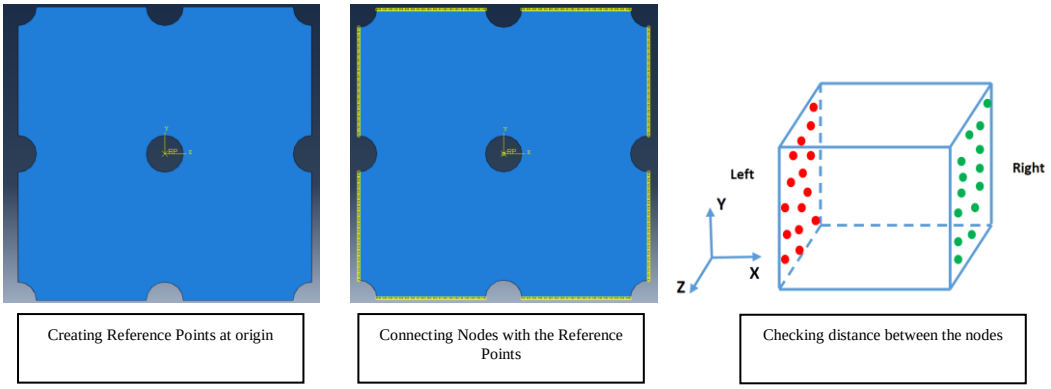

Figure 3.7 Logic to Connect nodes with Reference points

4. Once the PBC has been applied we have to give the dimensions of the plate which is 10 x 10 in terms of coordinates as mentioned in (Appendix A.1). Finally, the displacement of reference points has to be given using coordinates to initiate the movement of the respective nodes when the job has been run which will give the result shown in Figure 3.8 with a low computational time of 1 minute (it can change based on various conditions like size of model, shape of patterns, mesh size, load applied).

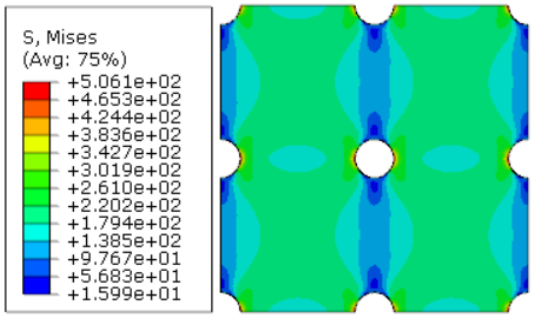

Figure 3.8 A 10 x 10 mm Plate Simulated in Abaqus with PBC

3.1.2.2. Validation and Comparison of Porus structures with PBC.

After understanding the concept of Periodic boundary conditions and implementation in Abaqus. We are going to validate numerically "Farhad Javid's et al." Reference [1] to authenticate our procedure which will support our development of new shape developments using the same approach.

Model Specification

Author fabricates dogbone samples of 90 x 25 mm shown in Figure 2.1 in chapter 2 for experimental purposes and obtained the same results using Finite element analysis in Abaqus using PBC by considering a 10 x 10 mm 2D section to reduce computational time as explained previously. The Material properties are of stainless steel SS316L with a modulus of elastic 193,000 MPa, Poisson's Ratio 0.33 and Yield strength of 205 MPa. Based on Reference [1] we

have designed circular shape, S shape and Ellipse shape with 3 aspect ratios maintaining the same porosity of 5 %.

Boundary Conditions and Meshing Parameters

As discussed above we are going to apply Periodic boundary conditions with Monotonic tensile load with applied strain 0.001% in the vertical direction which infers that the length is 10mm, so the corresponding displacement is 0.01mm. Similar to the Reference [1] the element shape is Quad free with standard quadratic CPS8 element type applied under plane stress condition. In section a &b we are going to apply these boundary conditions to validate authors results.

a) Validation and Shape Influence on Von Mises Stresses

In this case, the main parameter considered by the author is the normalized stresses as their motive is to increase the life of the plate with circular holes based on Reference [1]. Hence, they have replaced them with S-shaped patterns to reduce these stresses.

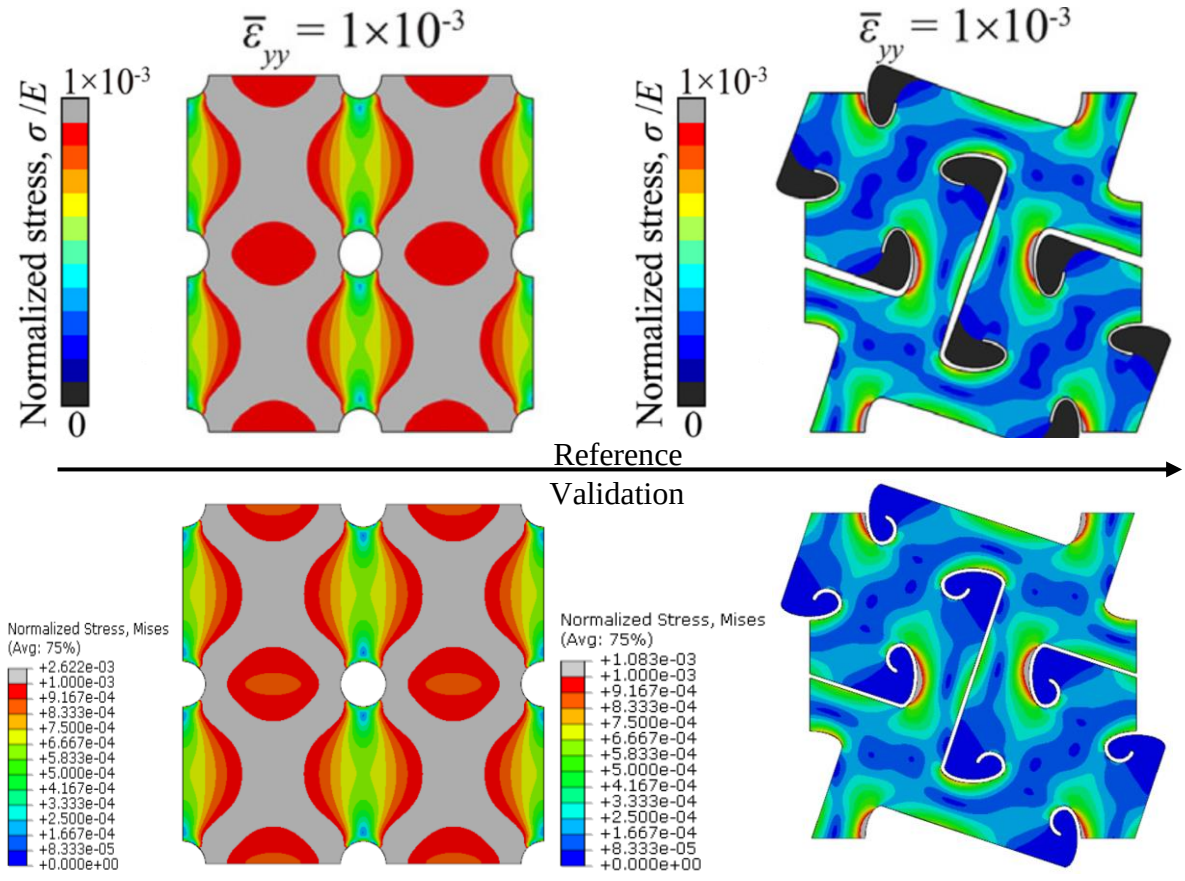

Figure 3.9 Numerical analysis and Validation: Distribution of Von Mises stress (normalized by the bulk material's elastic modulus E) for circular (left) and S-shaped (right) holes

As we can observe from Figure 3.9 our numerical analysis is a perfect match with authors results as per the Reference [1]. We have also normalized the Von Mises stresses by dividing

the Von Mises stresses with a modulus of elasticity based on authors approach to observe the yield area which can influence crack propagation. With the results shown in Figure 3.9, we can clearly see that the maximum normalized stress of S shape which is 58.6 % lower than the circular shape. Also, from the contour plots, we can observe that with circular holes the deformation mechanism is stretching, while in the S-shaped hole sample it is mostly rotation of the domains defined by the pores, which also results in a negative Poisson's Ratio. We can witness the mechanism that results in this remarkable behavior and finds that both the deformation mechanism and the way cracks propagate change in the S-shaped pores. More specifically, while large portions of the material are highly stretched in structures with circular pores, in the case of S-shaped holes, the majority of the structure experiences low-stress values as the deformation is found to induce the domain rotation between neighboring holes. As a result, the cracks initiated at the concentrations of stress along the S-shaped pores are trapped in regions of low stress and propagated at a significantly lower rate based on Reference [1]. When we compare the displacement plots in Horizontal & Vertical directions (U1 &U2 respectively) of both the shapes in Figure 3.10.

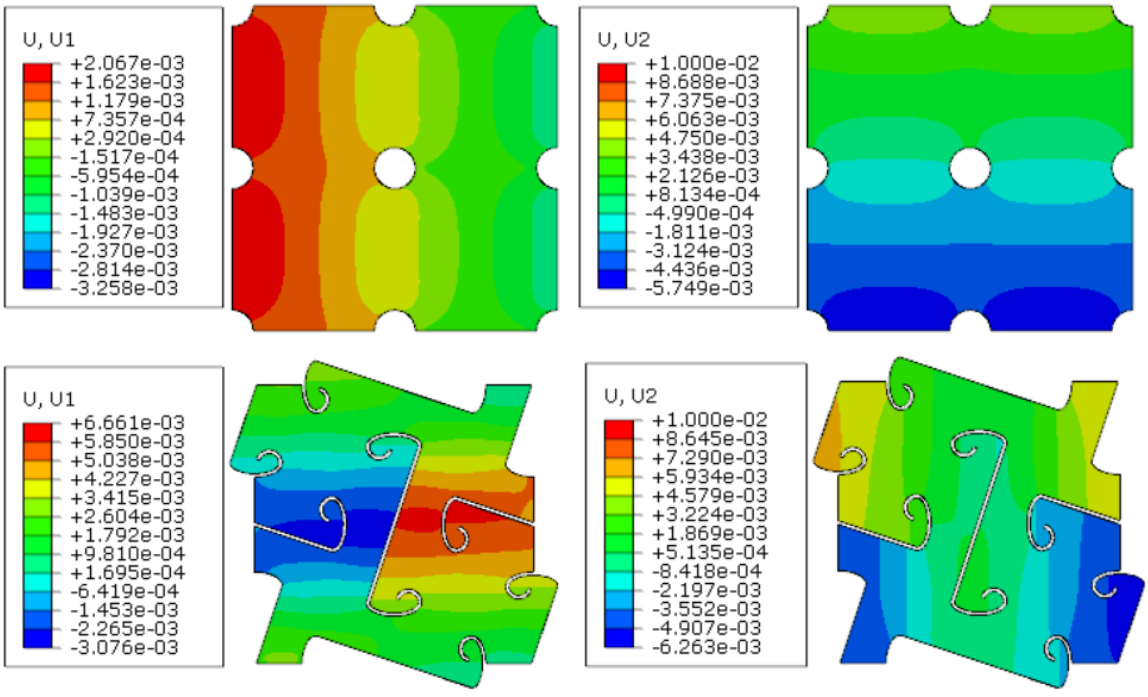

Figure 3.10 Displacement plots of Circular shape(top) and S Shape (bottom)

The maximum displacement of circular shape in the Horizontal direction (U1) is 0.002067 mm and 0.01 mm in the Vertical direction (U2) which is the direction of loading. Similarly, the maximum displacements of S shape in Horizontal & Vertical directions are 0.006661 mm and 0.01 mm respectively. So, we know through case study 3.1.1 displacement in the Horizontal

direction can detect the auxetic behavior of metallic perforated sheets. In this case, we have an increase of 222% in maximum displacement in the Horizontal direction by S-shaped plate when compared with the circular shaped plate based on the displacement plots in Figure 3.10. Which means that replacing S shape not only reduces stresses of the plate but enhances its previous behavior by adding auxetic property. This can be authenticated by the poisons ratio value which is -0.67 of S Shape pattern and 0.326 of the circular patterns which prove that the S-Shaped plate exhibit auxetic behavior with better load bearing capabilities compared to the circular shaped plate.

b) Validation and Aspect Ratio Influence on Von Mises Stresses

The second part of Reference [1] is the influence of aspect ratio on the distribution of stresses while maintaining the same porosity level. Author has altered the circular shape into three different aspect ratios to analyze the behavior of the stresses in a 10 x 10 mm plate using PBC described in section 2.2. So physically when the aspect ratio of a circle is changed it transforms into an ellipse.

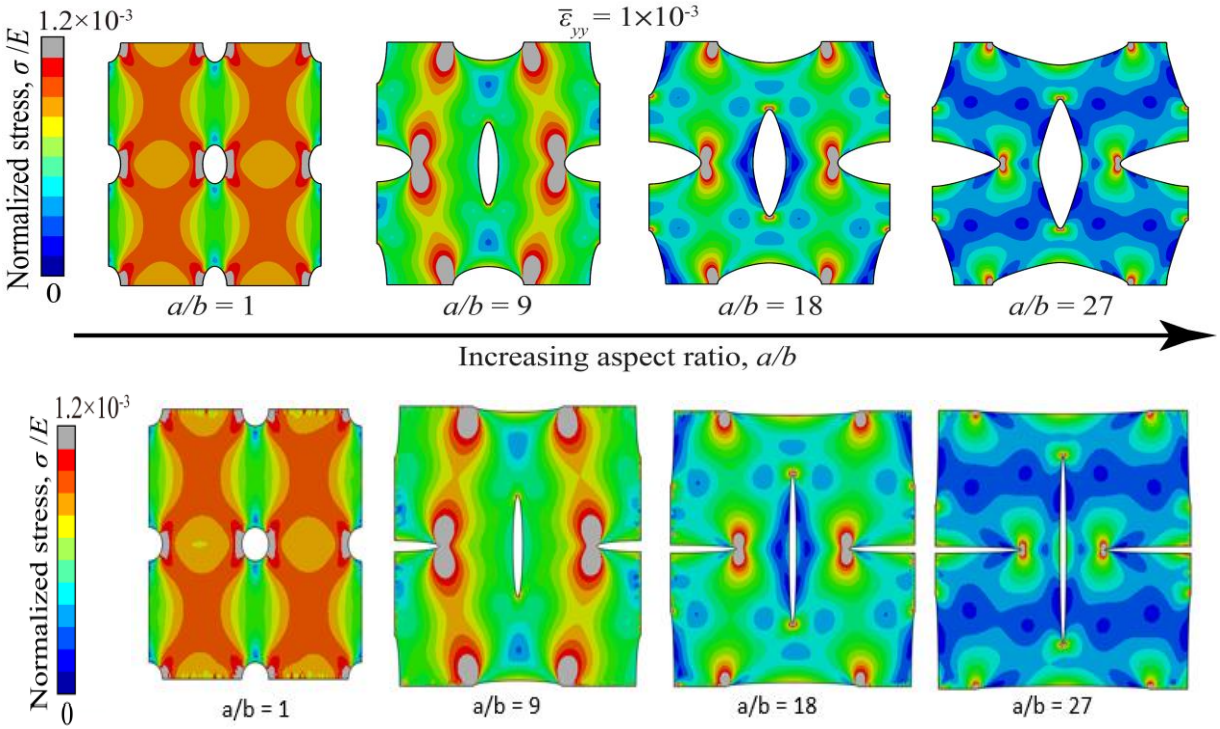

Figure 3.11 Numerical analysis and Validation: Distribution of Von Mises stress (normalized by the bulk material's elastic modulus E) for different Aspect ratios of circular pattern with Reference (Top) and Validation (Bottom)

According to Figure 3.11, a/b is the ratio between the two major axes of the shape which defines the aspect ratio of the pattern. Hence a/b ratio of the circle is 1 and based on Reference [1] we

have validated three different aspect ratios which are a/b=9, a/b=18 and a/b=30 respectively. Further increase of aspect ratio will make the ellipse tips very sharp which are prone to increase stress concentration factor according to Reference [1]. Based on numerical analysis results the author indicates that as the aspect ratio of the ellipses increases, the stress pattern in the structure changes. The pores are actually found only to locally perturb the displacement field in the case of circular holes so that the displacement field typical of the bulk material can be easily noticed. In comparison, the elliptical holes array is found to affect the displacement field considerably, thus disturbing the linear distribution. We can also discover the effect of aspect ratio on auxetic behavior of plates by observing the displacement plots in the Horizontal direction (U1) in Figure 3.12.

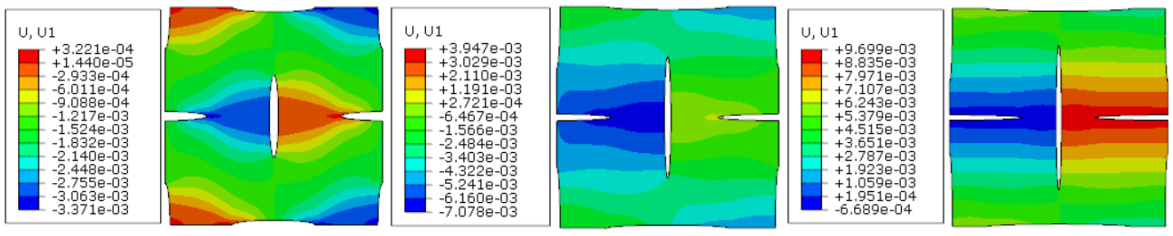

Figure 3.12 Displacement plots in X Direction (U1) of Ellipse with different aspect ratios

As discussed previously we have obtained displacements in the Horizontal direction (U1) which are can be observed in Figure 3.12. So, when comparing the maximum Horizontal direction displacement with the circular shape we have obtained a change in the percentage of displacement to determine the influence of aspect ratio on poisons ratio. For a/b=9 it has a decrease of -84.4% in maximum displacement comparatively than circular shape displacement hence it doesn't exhibit auxetic behavior, further there is an increase of 90.95% in maximum displacement in the Horizontal direction when the aspect ratio is increased to a/b=18 obtaining a Poisson ratio value of -0.39. Finally, when the aspect ratio is reached to a/b=27 the maximum displacement has increased to a staggering 369.23% achieving the Poisson ratio value of -0.75 which is the highest when compared to other aspect ratios. With this, we have demonstrated that by changing the aspect ratio of voids, the Poisson ratio can be effectively controlled. The structure is characterized by positive values of the Poisson ratio for low aspect ratios. However, as the aspect ratio increases the Poisson ratio's value monotonically decreases and becomes negative. They report an assessment of the Poisson ratio as a function of the pore aspect ratio in their study. As a function of aspect ratio, they maintained the porosity and modified the shape. The effective Poisson ratio is almost the same as the bulk material at aspect ratios close

to 1. The results show clearly that the aspect ratio a/b of the holes has a strong impact on the structure's lateral contraction/expansion. Significant auxetic behavior could be produced in low porosity metals if the ratio of void aspect a/b is sufficiently large. Hence, The results confirm that the shape aspect ratio can be effectively used to design structures with low porosity and the negative value of Poisson's Ratio. The high aspect ratio ellipses lead to the material characterized by a large negative value of Poisson's Ratio based on Reference [1].

Comparison of Von Mises Stresses and Poisson's Ratio

Based on the validation in section a and b above we are going to compare the results of the numerical analysis to conclude authors study based on Reference [1]. Hence, we verify that if the circle shape is replaced with ellipse shape & S shape of aspect ratio a/b = 27 will have increased load bearing capabilities with additions of auxetic property.

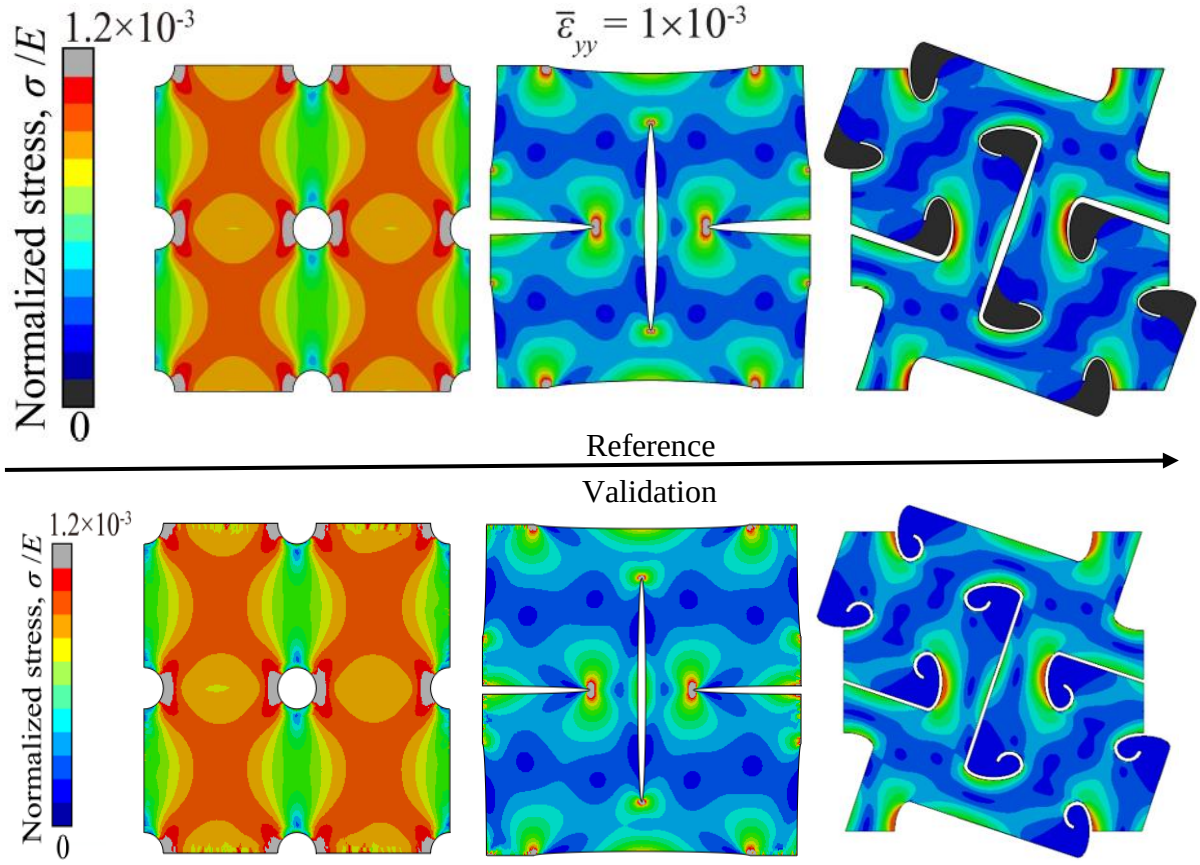

Figure 3.13 Normalized Stresses of 10 x 10 mm plate with 3 different shapes

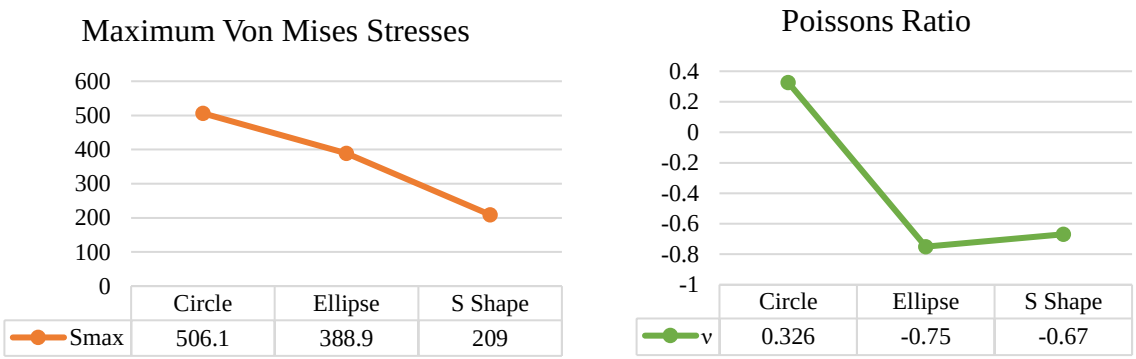

Graph 3.2 Plots describing Maximum Von Mises stresses and Poisson's Ratio of 3 different patterns

Based on the numerical analysis in Figure 3.13 we have compared them graphically in graph 3.2 to validate the author's study. With the plots, we can observe that the S-shaped pattern has the lowest Maximum Von Mises stresses out of the other two shapes. Even if the structures with elliptical and S-shaped holes are characterized by qualitatively similar behaviors the high local stresses around the tips of the elliptical holes result in a higher value for Von Mises Stresses. Also, in the case of elongated elliptical holes, most of the structure experiences low values of stress when compared to a circular shape and the deformation is found to induce rotation in the domains between holes. We also note that, as for the case of the S-shaped holes, the stress is concentrated around the tips of the ellipses. Such localized stresses are higher for the elliptical holes than for the S-shaped pores. This is because the S-shaped pores are designed to minimize the curvature at stress concentrated points as per the Reference [1]. When we move on to the Poisson's ratio values in Graph 3.2 the ellipse shape and S shape both exhibit auxetic property. Hence replacing circular patterns with S shape and Elliptical patterns can greatly increase the fatigue life of the material and can exhibit auxetic behavior in future applications to enhance productivity. The proposed structures are also characterized by low porosity, making them suitable candidates for many components of gas turbine engines with cooling requirements. These components will benefit from the proposed design, since it will greatly increase the fatigue life while preserving their low-porosity and, consequently, their cooling performance described by the author in Reference [1].

4. SHAPE STUDY AND TOPOLOGY OPTIMIZATION

All the discussion above was focused on designing new pores shapes which will have better stress field distribution and can show auxetic behavior based on a specific application which demands such enhancement. Based on references [2], [5-8] we have chosen shapes which can be used to investigate and optimized. As discussed in section 3.1.2 we are going to apply the same boundary conditions with the similar procedure on the new shapes with the aim to reduce Von Mises stresses and enhance auxetic property depending on the pore shape behavior.

Model Specification

All the shapes have been designed on a 10 x 10 mm plate with the center to center distance of 5 mm with 2-dimensional perspectives as it reduces numerical simulation time to analyze shape behavior. Based on Reference [1] the adopted material is SS316L stainless steel with a modulus of elasticity about 193,000 MPa, Poisson's Ratio of 0.33 and Yield strength of 205 MPa. In our study, we have kept porosity constant depending on the design criterion we are analyzing and comparing the pores which are discussed in section 4.2.

Boundary Conditions and Meshing Parameters

As discussed above we are going to apply Periodic Boundary conditions (section 2.2) with monotonic tensile load with applied strain 0.001% in the Y direction which infers that the length is 10mm, so the corresponding displacement is 0.01mm. Based on Reference [1] the element type is CPS8 (Quad free 8-node quadratic plane stress element) applied under plane stress conditions. Applying these meshing parameters for the 2D void patterns will produce the values for the measuring parameters discussed below.

Measuring Parameters

Based on References [1-3] we have considered four parameters which can be considered as the judging factors. The parameters are the following:

a) Von Mises Stresses (S_{MAX})

Von Mises stress is a value used to determine if a given material will yield or fracture. The Von Mises yield criterion states that if the Von Mises stress of a material under load is equal or greater than the yield limit of the same material under simple tension which is easy to determine experimentally, then the material will yield. Using Abaqus we will obtain Von Mises stresses directly which will be used to calculate stress concentration factor and assist to comment regarding the stress field of the pattern.

b) Stress Concentration Factor (K_t)

To calculate the stress concentration factor, we have applied the periodic boundary condition on a 10mm X 10mm plain 2D structure as shown in Figure 4.1 and calculated the Von-Mises stress of the plain sheet. The value was 193MPa. Then to verify the same we have applied the same on a plate with a circle in the center and we have obtained the value of stress concentration factor as 2.9 ($K_{t,\ hole}$: 560/193) which is very close to 3. Thus, the procedure for calculating the stress intensity factor is validated.

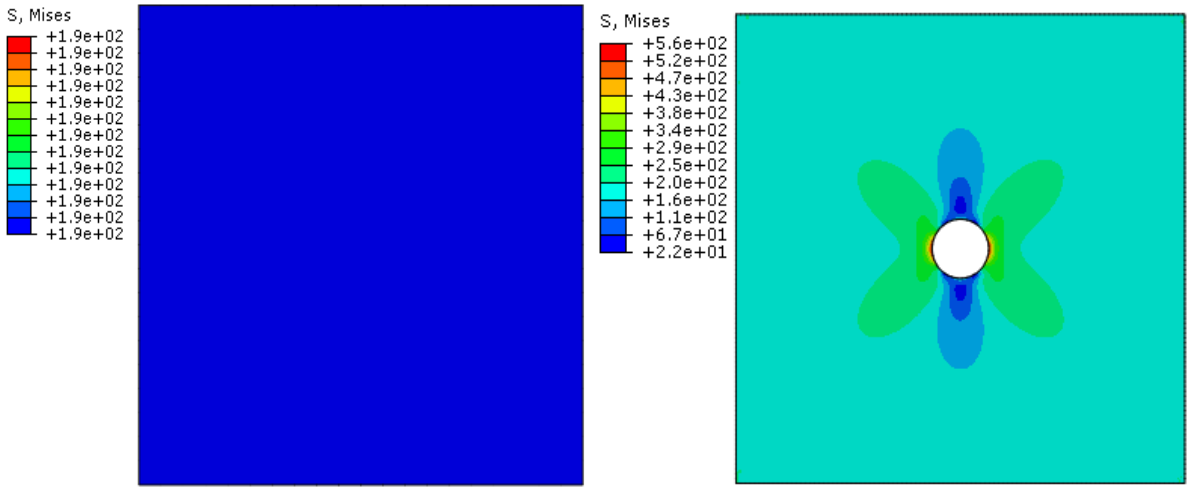

Figure 4.1 Von Mises Stresses of the Plane sheet and Plate with Hole

c) Poisson's Ratio (v)

Poisson's Ratio is a measure of the Poisson effect, the phenomenon in which material tends to expand in directions perpendicular to the direction of compression. Conversely, if the material is stretched rather than compressed, it usually tends to contract in the directions transverse to the direction of stretching. But in case of auxetic behavior, when stretched the perpendicular sides of the material expand to the applied tension, and when compressed, they shrink in the two directions perpendicular to the applied compression as discussed in section 2.1. Hence, they have negative value in Poisson's Ratio. We have calculated Poisson's Ratio of our model based on the distance they have stretched or contracted in Figure 4.2 X & Y are the length of the plate before they are stretched and dX & dY are lengths after they are stretched then the Poisson ratio will be:

$$\epsilon_x = (dX - X)\ ;\ \epsilon_y = (dY - Y)$$

$$\text{Poisson's Ratio: } \nu = \frac{-\epsilon_x}{\epsilon_y}$$

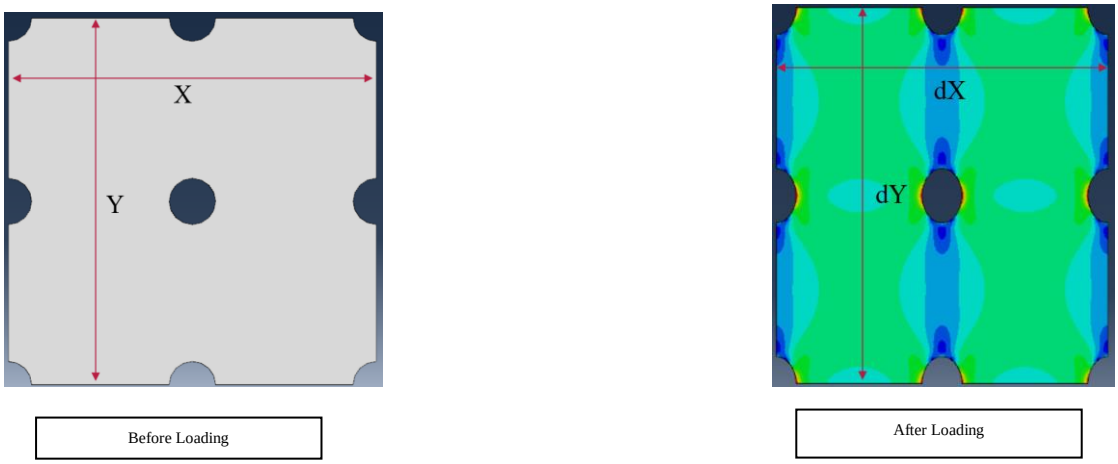

Figure 4.2 Poisson's Ratio Computation

d) Critical Area (%)

The Critical Area is the percentage of the area which is stretched above the yield strength of the material. This Critical Area of material which bears most of the load applied on the material becomes weaker over time and can initiate cracks which can propagate from one pore to another. Hence, measuring Critical Area we can predict crack propagation and take appropriate measures to reduce them. We have demonstrated the calculation of the Critical Area in Figure 4.3 where we have limited the Von Mises stresses between 205 MPa and 0 MPa. Due to which we can see the grey area near the circular shapes prone to initialization of cracks, hence the area is critical and should be as low as possible.

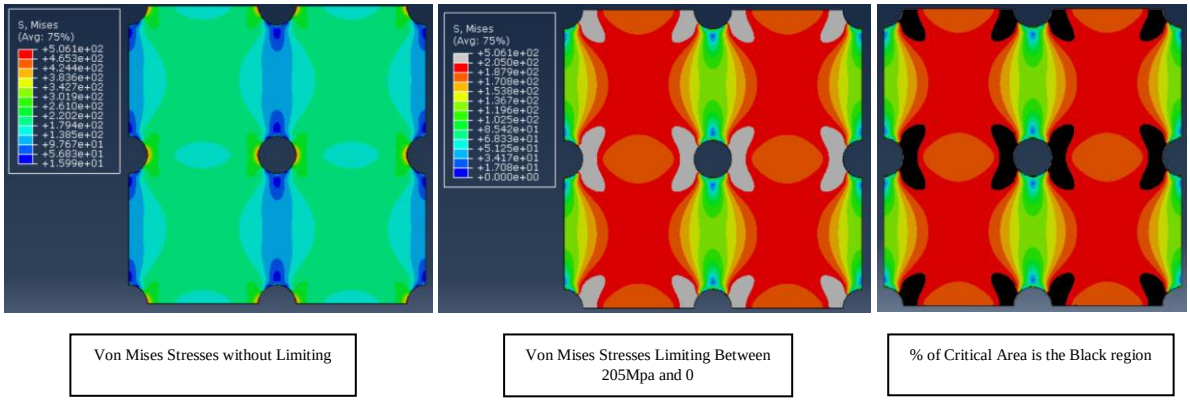

Figure 4.3 Critical Area Computation

Hence, the above-discussed parameters will be calculated for all the shapes which we have considered for our study. According to the values of parameters, we can decide the suitable combination of shape with the approximate arrangement, appropriate porosity and position. We will be plotting the values of parameters in graphical formats in upcoming sections for comparison purposes and conclude the best combination of shapes for specific applications.

4.1. SHAPE SELECTION

Shape selection was performed based on references [2], [5-8] due to reasons depending on the shape, material, and behavior. We have considered six shapes for numerical analysis categorized into thin structured shapes (Figure 4.4 a,b,c) and thick structured shapes (Figure 4.4 d,e,f) to maintain porosity for a valid comparison.

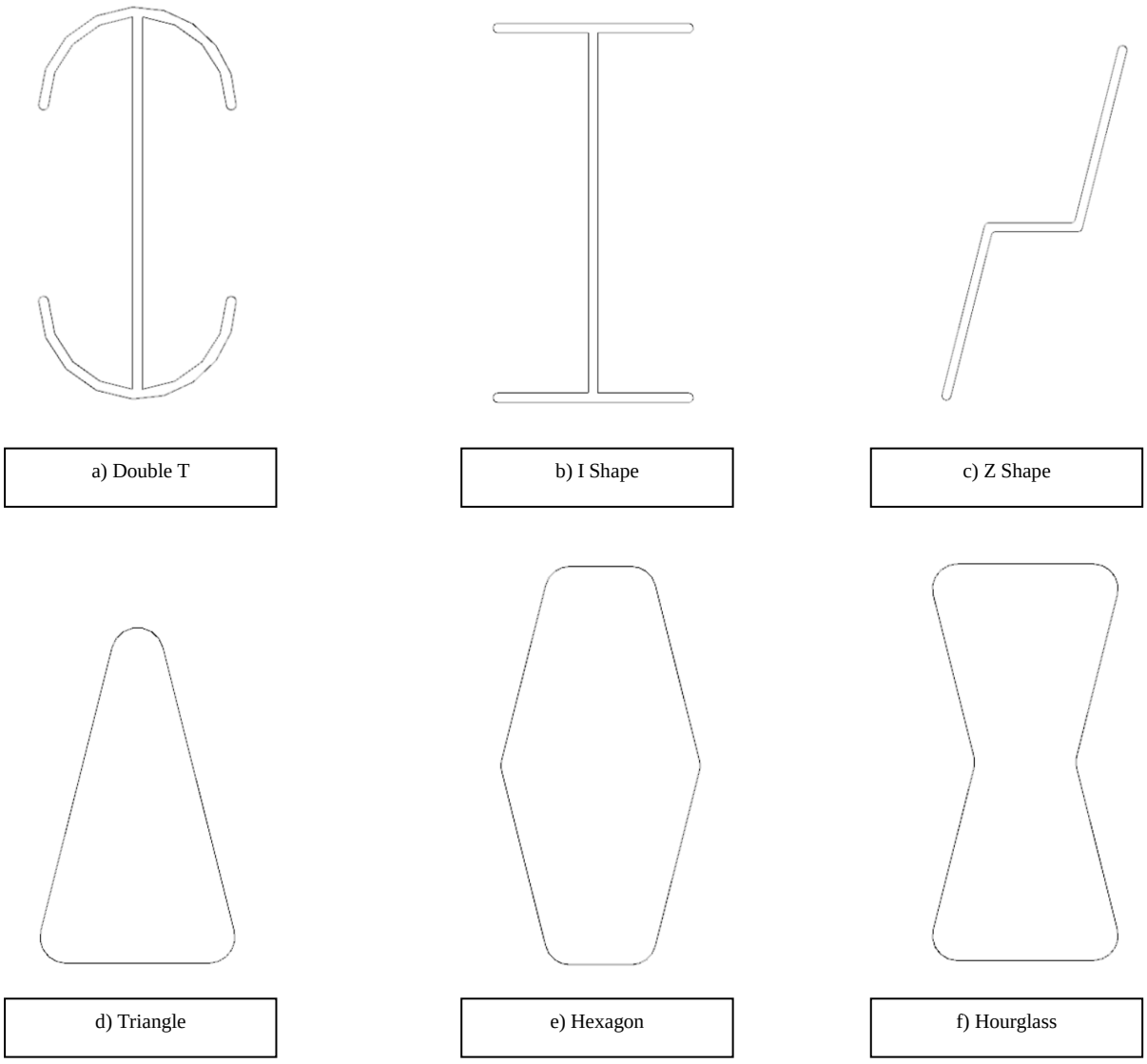

Figure 4.4 Selected Shapes for Numerical Analysis

a) Double T

This shape is selected based on the reference [2] which we had also discussed and verified in section (3.1.1). It can attain auxetic behavior with reduced Von Mises stresses. Hence, we are going to observe its influence on measuring parameters discussed above on various design conditions. Also, topology optimization will be performed to check the potential to improve the mechanical properties of the metallic plates.

b) I Shape

According to reference [5], a novel class of mechanical metamaterials created through the introduction of I shaped perforations were proposed and investigated with respect to their potential to exhibit a negative Poisson's Ratio. As they have performed it on metamaterials which are composites of metals or plastics, we designed I shape on the metallic plate to examine similar behavior.

c) Z Shape

Based on reference [6] the author conveys that 2D auxetic materials with the isotropic response can be easily realized by perforating a sheet with elongated cuts arranged to form a periodic pattern with either six-fold or three-fold symmetry. So, the cut they have chosen was a Z cut pattern which we have embedded on our model to enhance our mechanical properties and optimize if necessary.

d) Triangle

The reason for choosing a Triangle is to understand the influence of the edges on the stress concentration factor in metallic plates and finding better design solutions to optimize it. The effect of bluntness, the rotation angle of the hole, hole size, and hole shape as significant parameters on stress distribution around the holes are studied in reference [7]. Thus, we choose Triangle to observe Von Mises stress distribution when Periodic boundary conditions are applied.

e) Hexagon

Similarly, like the Triangle shape author of reference [7] also included Hexagon to his analysis to observe the influence of stress concentration factor when edges are increased and rotated. The results presented by the author indicate that due to uniaxial loading, the stress concentration factor can be significantly varied by changing the pattern shape, bluntness and rotation angle of the hole. The infinite plate containing square and hexagonal holes, for a wide range of bluntness, the desirable stress concentration factor is less than the desirable stresses of similar plates with a circular hole.

f) Hourglass

The inspiration of Hourglass shape was obtained from reference [8] where they have designed anti-tetrachiral and re-entrant honeycomb auxetic geometries on composite structures to observe auxetic behavior under the influence of temperature. But we are designing the Hourglass shape to achieve auxetic behavior under the influence of static loading on metallic plates.

4.2. INFLUENCE OF PERFORATIONS ON MEASURING PARAMETERS BASED ON DESIGN CONDITIONS

Based on the evidence reported in the references [1-8] we have tested the shapes described in section 4.1 with a set of design conditions which will give us the context to judge on the behavior of shapes and to comment on the best possible design combination. The load conditions and meshing parameters are discussed in section 4.1 which is the same for all the design conditions.

4.2.1. Increase in Size.

Size of the pattern is really an important factor to be considered while designing a perforated metallic sheet. To evaluate this condition we considered three different sizes values in which shapes are designed 2x2, 4x2 and 6x2 space respectively. Basically, they are small, medium and large sizes of shapes (Figure 4.5) are designed to observe their influence on the parameters when periodic boundary conditions are applied.

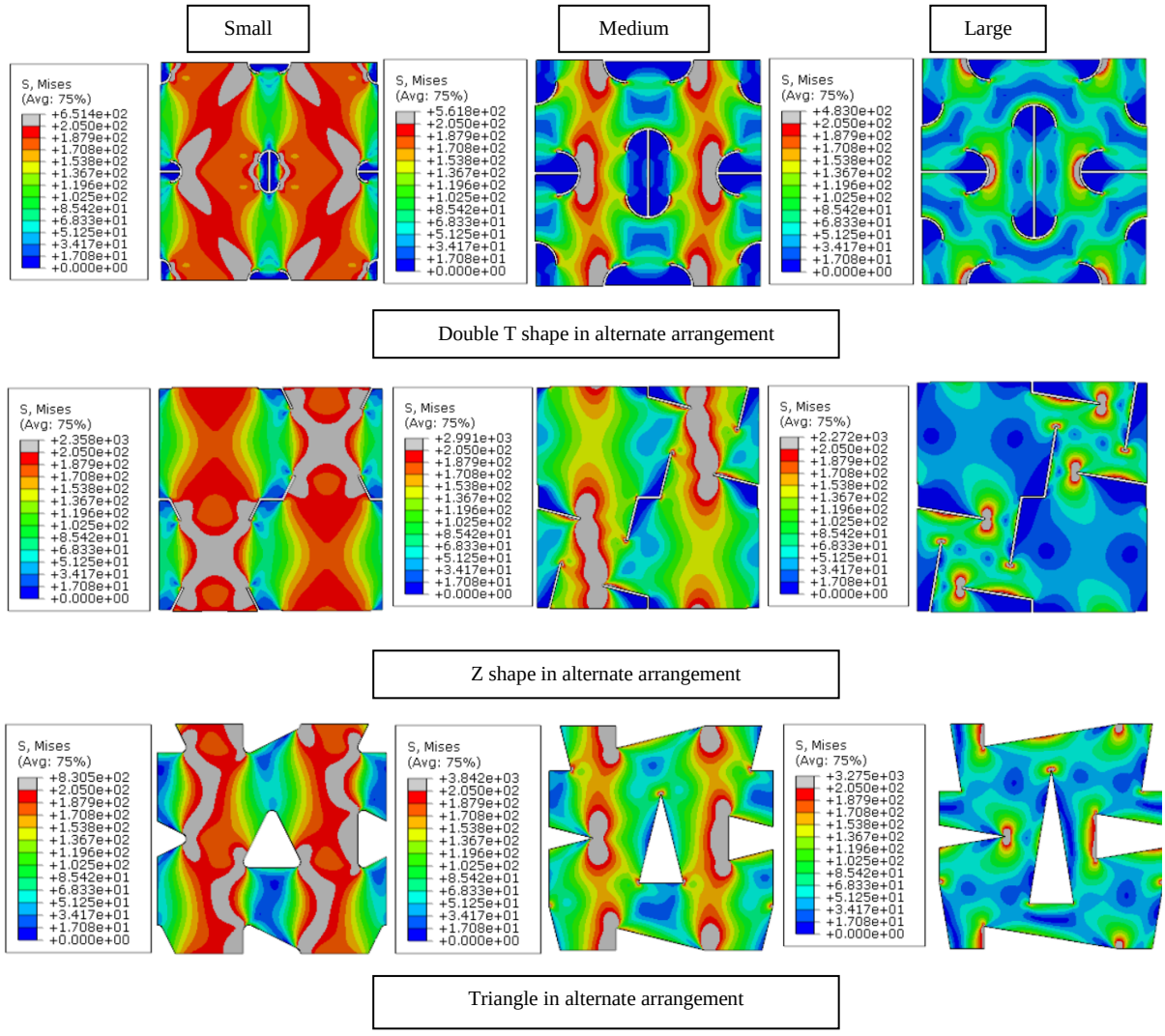

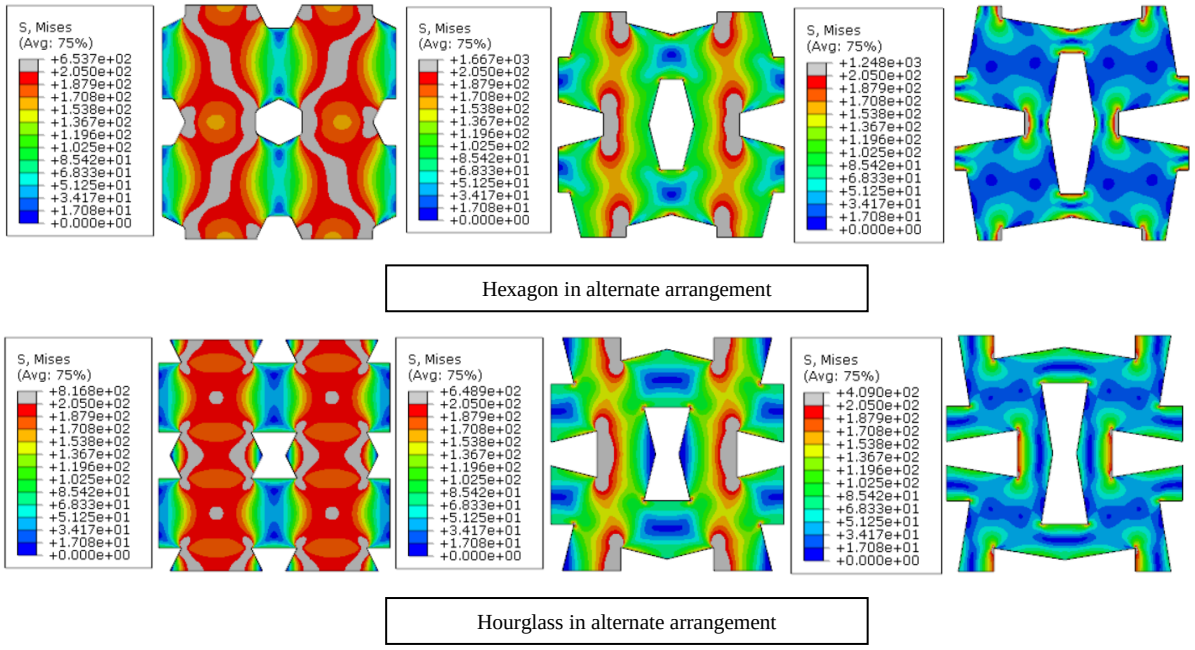

Figure 4.5 Numerical Analysis of shapes in different sizes

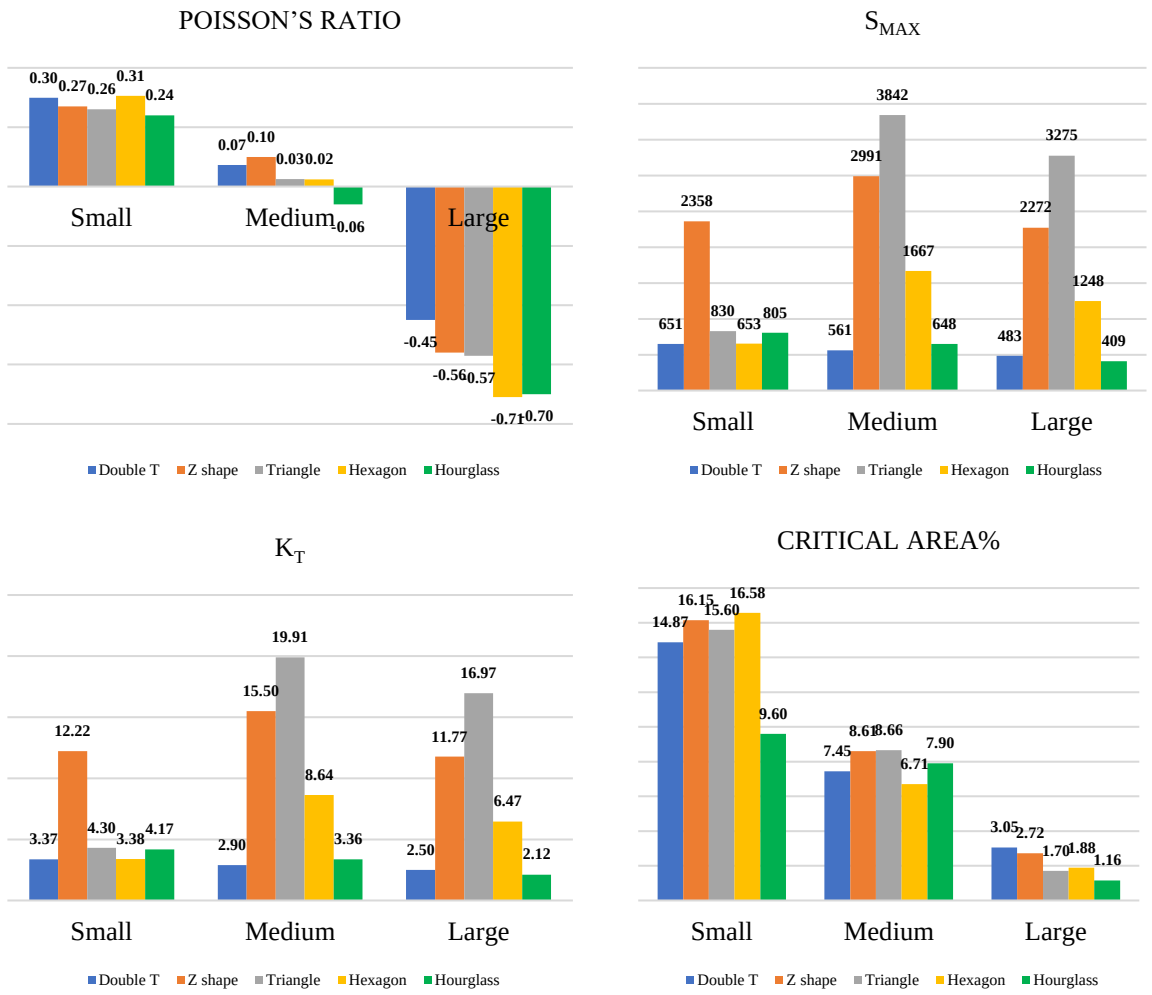

Graph 4.1 Bar Plots of parameters based on different sizes

Based on numerical analyses we have plotted the parameters in Graph 4.1 which we can use to predict the effect of size on the perforated metallic plate. When we observe the Poisson's Ratio value the large-sized patterns achieve most negative values when compared to small and medium size patterns. But large size patterns will be restricted to specific arrangements only when compared to small and medium-sized patterns. The best auxetic behavior in case of thin structured shapes is Z shape (Poisson's Ratio -0.56) and thick structured shapes were dominated by Hexagon & Hourglass shape (Poisson's Ratio -0.71 & 0.70 respectively).

Now if we analyze the stresses induced by the patterns the Z shape and Triangle shape induce very high stresses due to the sharp edges at the tips which increment the Von Mises stresses when size is increased based on the Graph 4.1. But in a large size, the Critical Area percentage is the least meaning that they are less prone to crack propagation when compared to small and medium-sized patterns. The best reliable shape in case of bearing static loads in case of thin structured shapes is the Double T shape and Hourglass shape achieved the least stress value in case of thick structured shapes. Hence, we can state that large-sized shapes can be applied on perforated sheets based on the application considered to achieve best auxetic behavior with least stresses, but if the arrangement of patterns is a priority then medium sized can be considered as they have respectable stress values with very less Poisson's Ratio values. We can now neglect the small-sized shapes as their parameter values are not reliable.

4.2.2. Influence of Arrangement.

The arrangement of patterns is greatly influenced by the direction of loading, as we are applying the load in the Vertical direction, we are going to analyze three configurations of arrangements considering medium-sized patterns which are Horizontal, Vertical and alternate configurations as shown in Figure 4.6. Based on this we can decide the configuration suited best when loading direction is known.

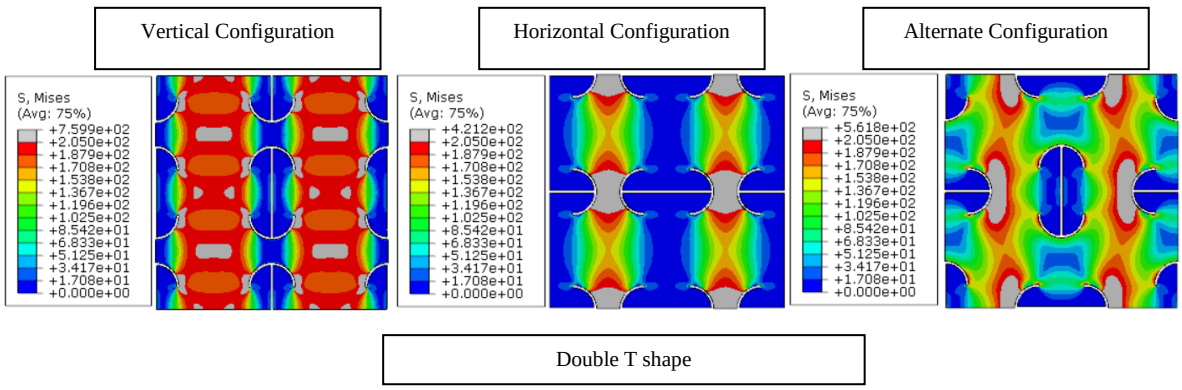

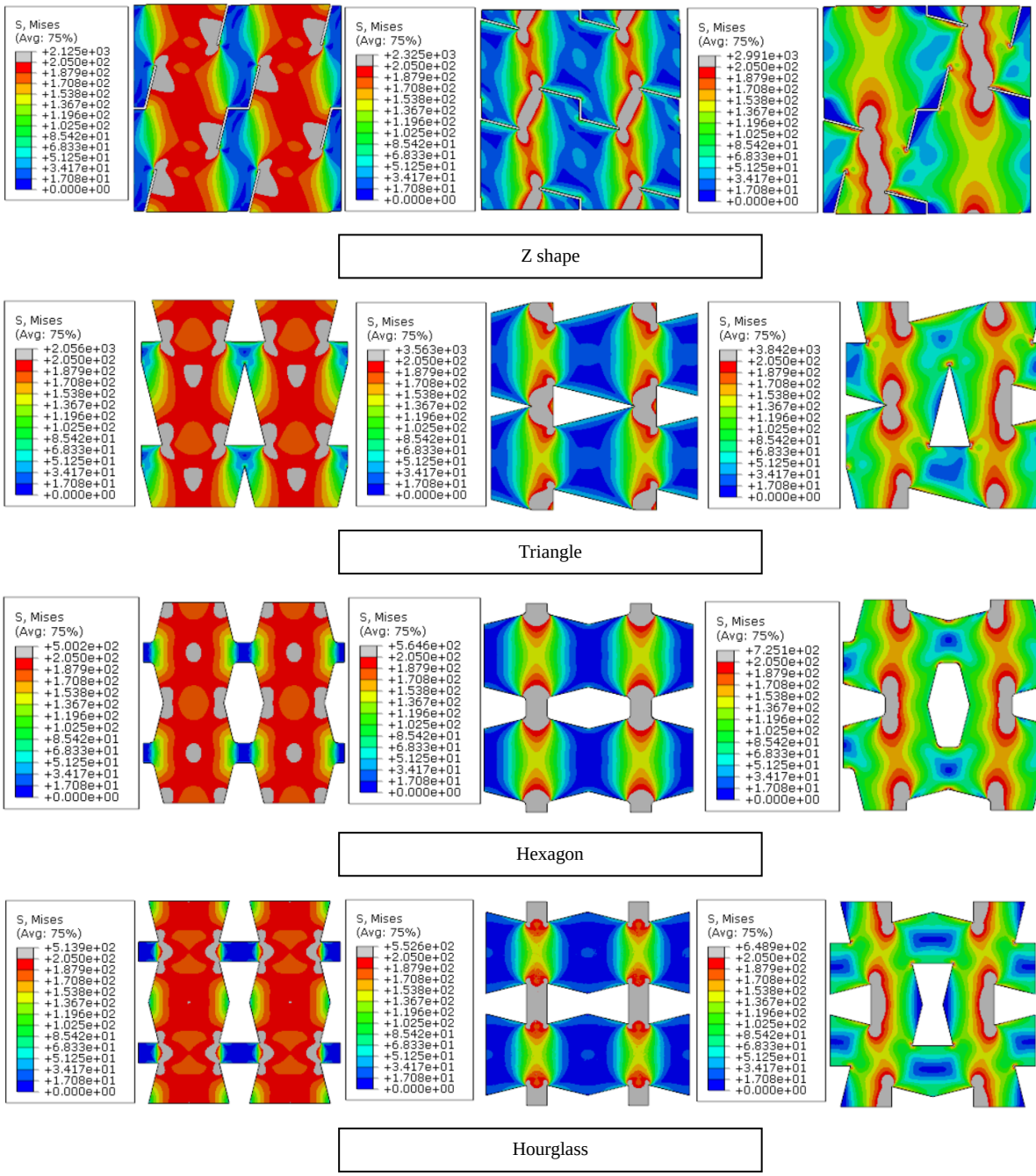

Figure 4.6 Numerical Analysis of shapes in different configurations

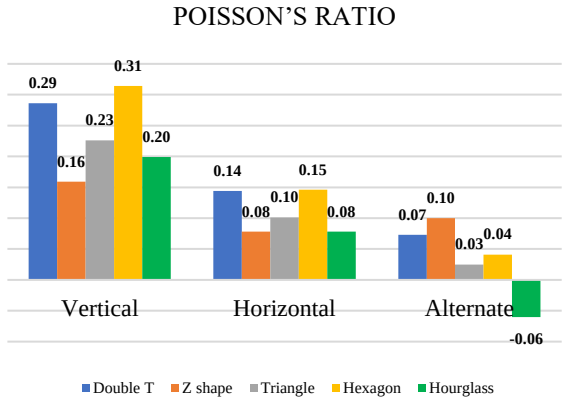

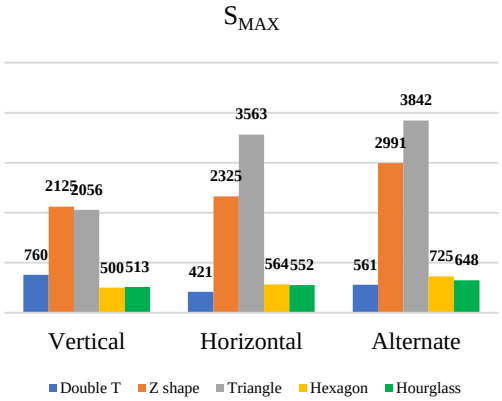

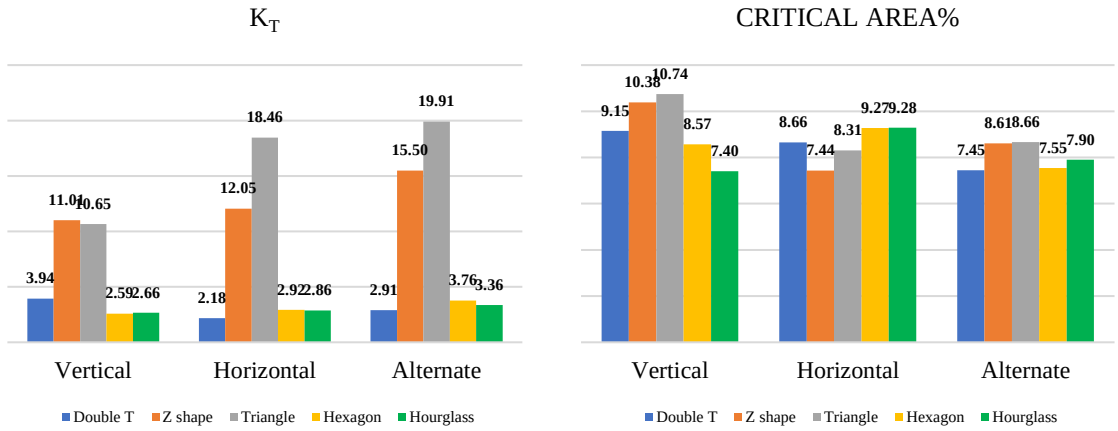

Graph 4.2 Bar Plots of parameters based on different configurations

Based on the numerical analysis on three configurations we have plotted the parameter values in Graph 4.2. We can observe the Poisson's Ratio plot which clearly depicts that alternate configuration gives the least Poisson's Ratio values when compared to other two configurations for most of the shapes except the Z shape which has lower value in a Horizontal configuration. The best auxetic behavior is achieved by the thin structured shape is the Double T shape which has Poisson's Ratio of 0.07 in an alternate configuration. In case of thick shaped structure, we have Hourglass shape with Poisson's Ratio of -0.06 which is best among the bunch demonstrating auxetic behavior.

When we observe in perspective of stresses Z shape and triangle has very high Von Mises stresses as well as stress concentration factor which increases from Vertical till the alternate configurations. The least stresses have been achieved by thin structured shape is Double T with a stress concentration factor of 2.18 and 8.66% of the Critical Area in a Horizontal configuration because it distributes the stresses Horizontally to the patterns nearby when compared to other two configurations. In case of thick structures shape, Hourglass shape presents the least Critical Area of 7.4% and a stress concentration factor of 2.66 which might be a little higher when compared to Hexagon shape which has stress concentration factor 2.59 in the Vertical configuration, but we can trade off with Von Mises stresses with a Critical Area for better stress field distribution.

Hence overall the configuration of the patterns depends on the shapes we choose based on the application we demand. In our study Double T, Hourglass and Hexagon shapes have the best results in all the three configurations.

4.2.3. Influence of Profile.

Based on the discussion above we have observed that with slight profile changes we can reduce Von Mises stresses in some shapes which have sharp edges. So, we have performed profile changes to four shapes namely Triangle, Hexagon, Hourglass and Z Shape with increased fillet size to remove sharp edges. We have considered medium-sized shapes with an alternate configuration for observing the change in parameters due to profile change as shown in Figure 4.3.

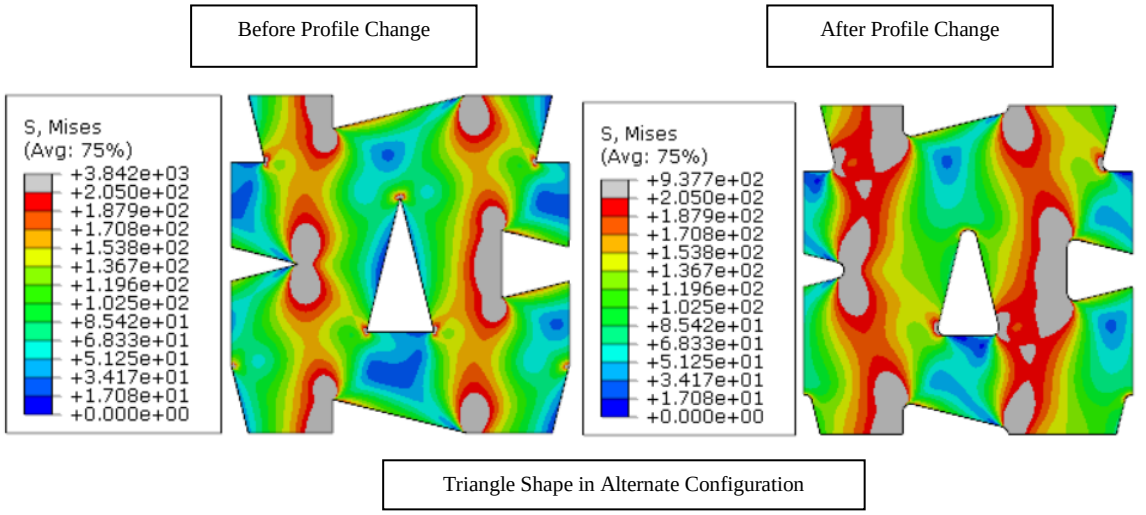

Triangle Shape in Alternate Configuration

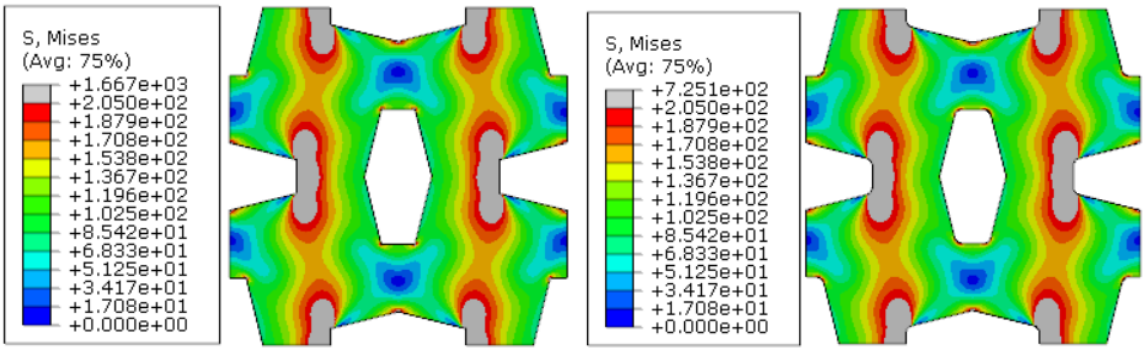

Hexagon Shape in Alternate Configuration

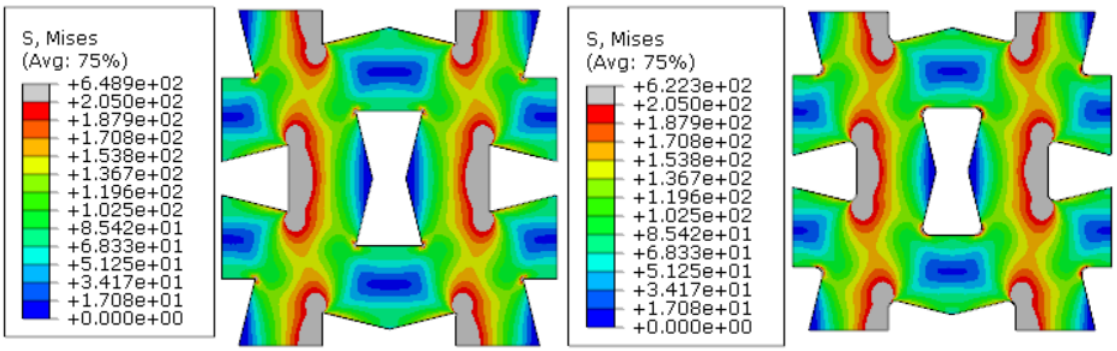

Hourglass Shape in Alternate Configuration

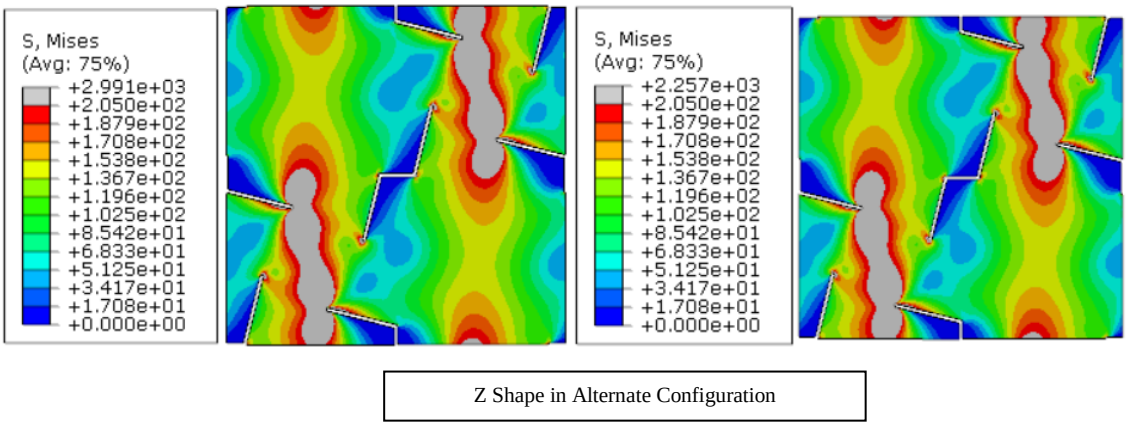

Figure 4.7 Numerical Analysis of shapes with Profile changes

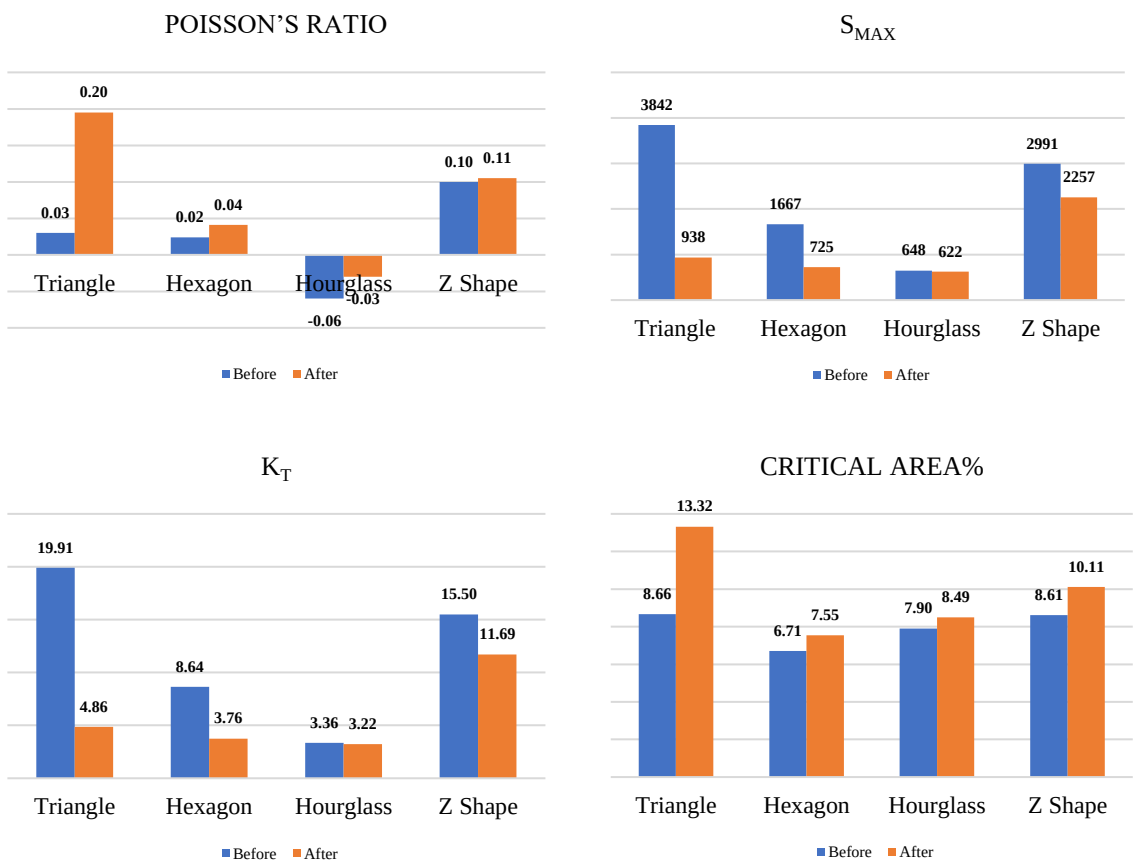

Graph 4.3 Bar Plots of parameters based on the Influence of Profile

Based on Numerical analysis of shapes we have chosen for Profile change we have obtained Graph 4.3 with measuring parameters. Based on the Graphs we can observe the Von Mises Stresses (S_{MAX}) and stress concentration factor (K_T) have a drastic difference when compared with older profiles, especially for Triangle, Hexagon, and Z shapes. Which means that adding bigger fillets can reduce the stresses influence in the metallic perforated sheets. But there is just a slight decrease in the Hourglass shape when compared with the older profile.

If we observe the Poisson's Ratio and Critical Area values, there is a significate increase due to the change in profile especially in Triangle shape when compared to other shapes. Which infers that shape edges have greater Poisson's Ratio values and lower Critical Area but with higher stress values. Hence, if stresses are more priority then adding bigger fillets will reduce considerable stresses with the sacrifice of lesser Poisson's Ratio value.

4.2.4. Influence of Rotation.

Rotating patterns in different angles can impact the parameters and distribution of stresses from one pattern to another. Hence, we have analyzed and compared our shapes in four different angles at 45^0, 90^0, 135^0 and 180^0 as shown in Figure 4.8. Based on this we can decide if the rotation of shapes is necessary for improvising our parameter values. In Figure 4.8 we have demonstrated only two shapes (Double T and Triangle) due to space considerations.

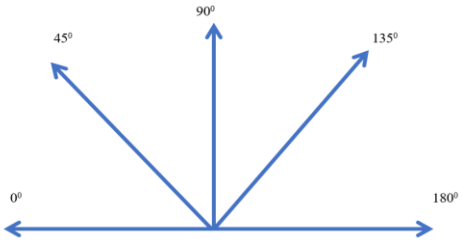

Rotation angles considered

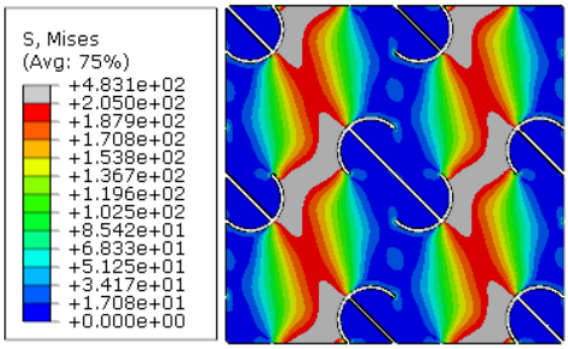

45^0 Rotation of Double T Pattern

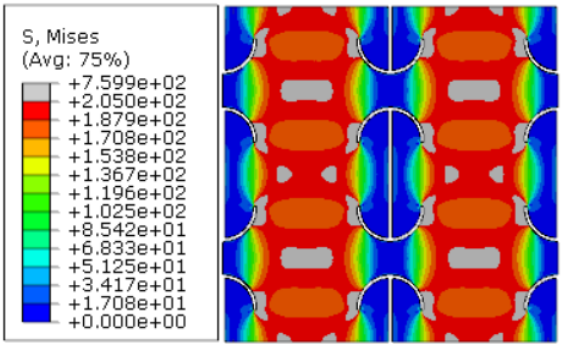

90^0 Rotation of Double T Pattern

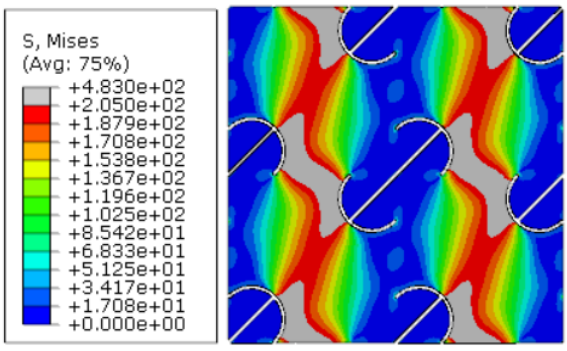

135^0 Rotation of Double T Pattern

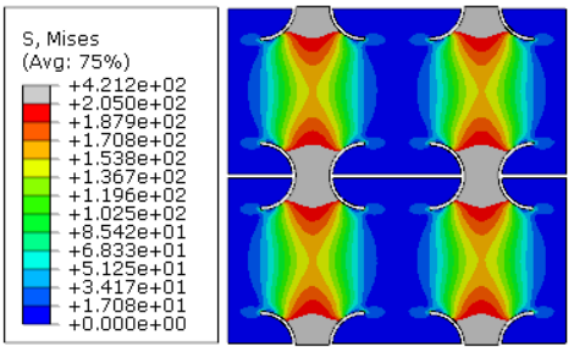

180^0 Rotation of Double T Pattern

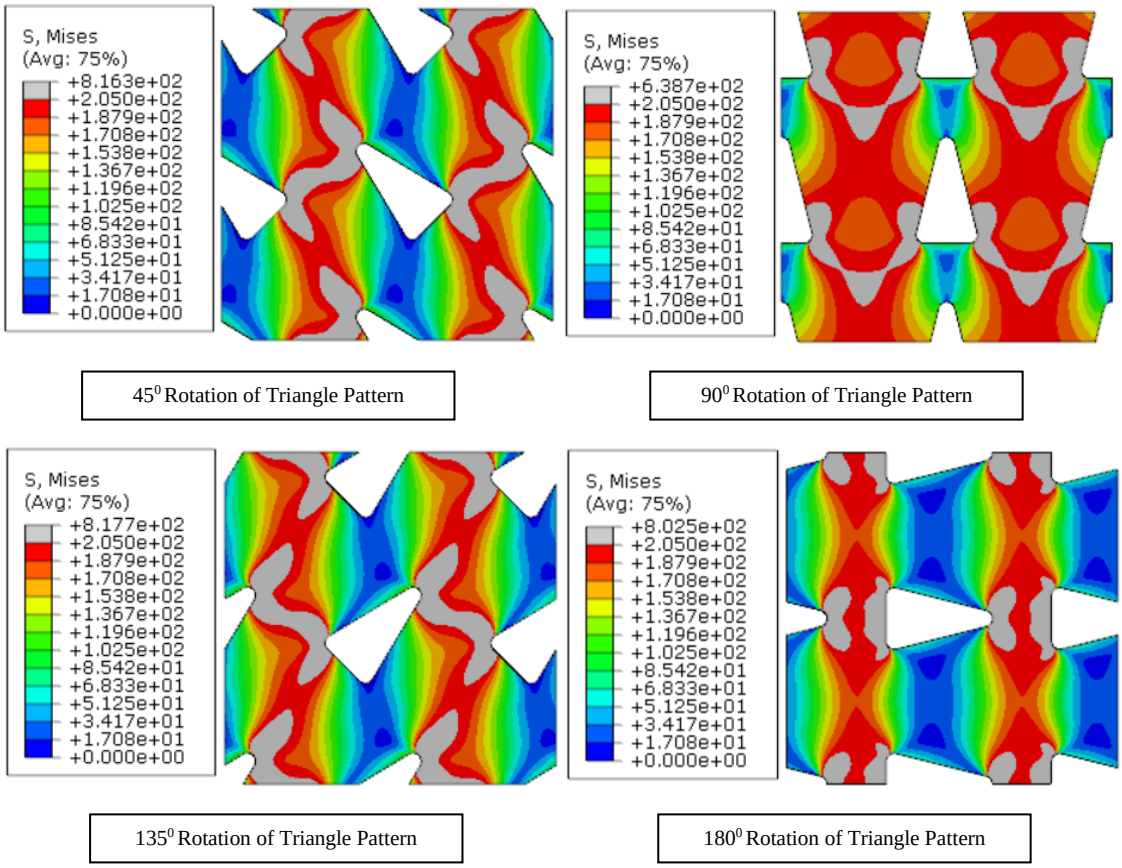

Figure 4.8 Numerical Analysis of shapes with Rotation of patterns

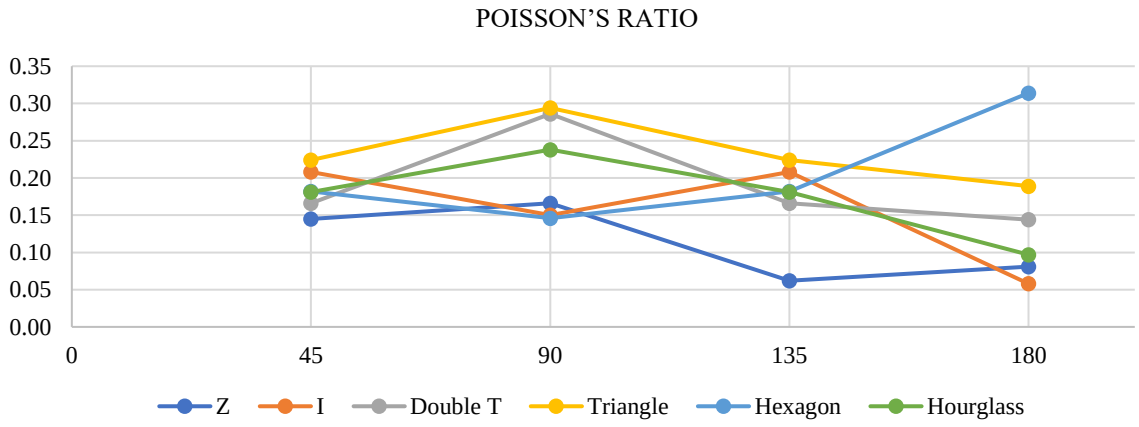

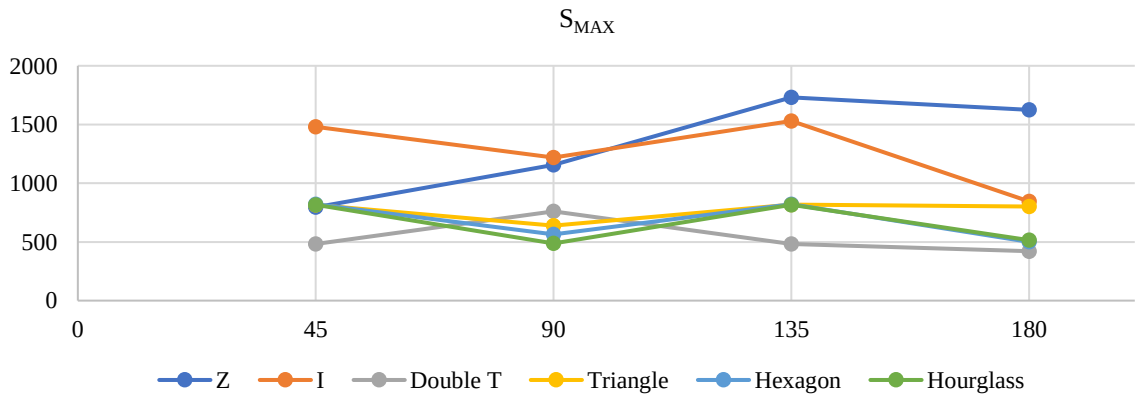

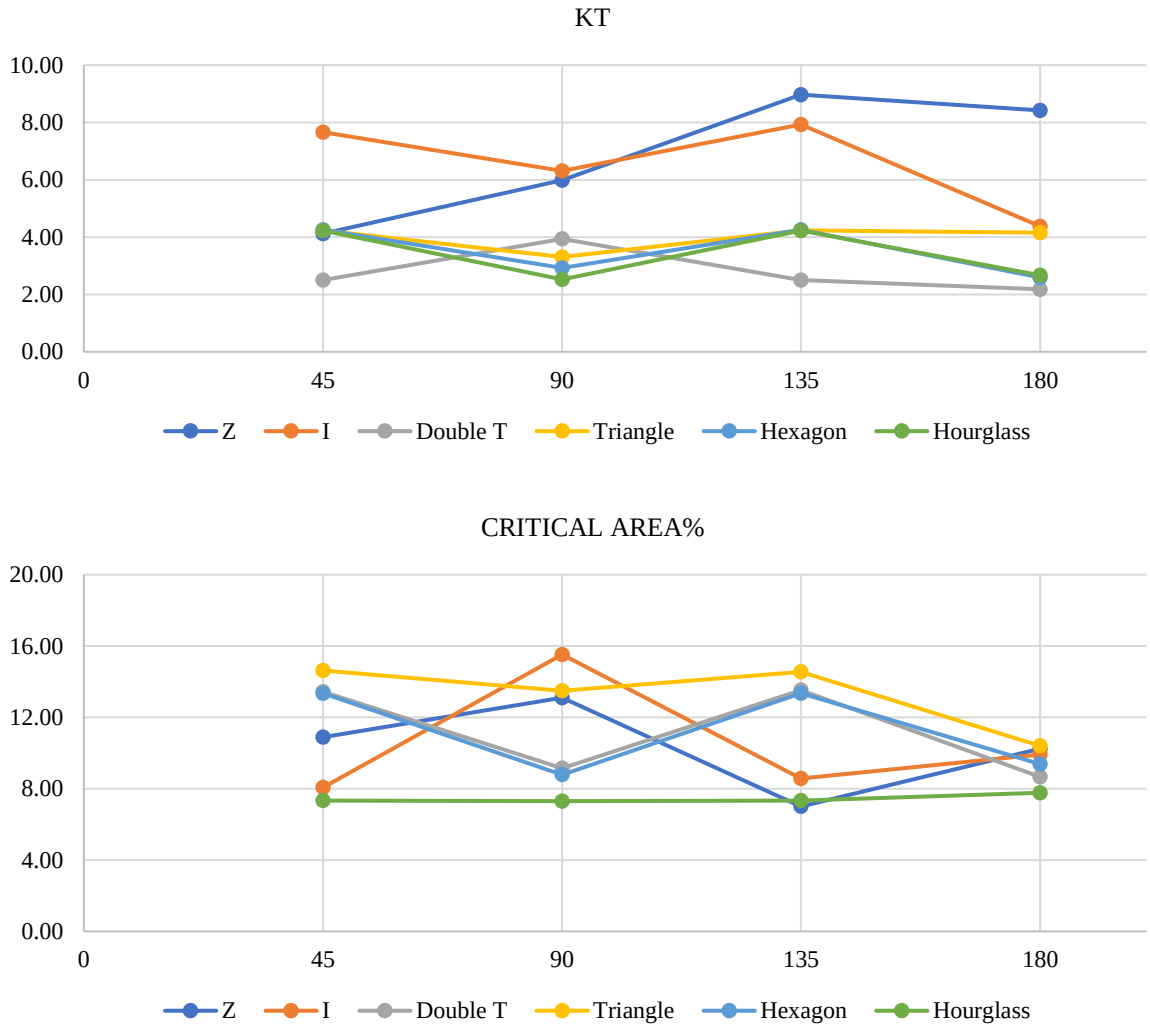

Graph 4.4 Plots of parameters based on the Influence of Rotation

With the parameter plots obtained above, we can see that except Z shape and triangle shape the values of 45^0 and 135^0 are identical for all the plots above as they are just mirror replicate of each other. Most of the shapes (except Z shape) have higher stress values at 45^0 and 135^0 angles because of the bridge of Critical Area between the edges are in an angular connection based on the stresses distribution in Figure 4.8 which induces more stresses than a straighter Critical Area as in 90^0 and 180^0 contour plots. Hence, when the gap between the edges of patterns can initiate cracks if they are placed in inclined angles for most of the shapes.

The Poisson's Ratio is lowest when we the shapes are placed in 180^0 angle for most shapes except for the Hexagon and Z shape. Hexagon shape has lower poisons ratio in 45^0 angles and Z shape has in 135^0 angle. So, angular placement of patterns is not recommended if the direction of loading is in Horizontal or Vertical directions.

4.2.5. Influence of Width between Patterns.

This design condition was considered to judge the behavior of stresses when we alter the width of the plate while keeping the height constant, which also means we alter the distance between pattern because of periodic boundary conditions. So, numerical analysis is performed in four different width conditions which are 3x10 mm, 5x10 mm, 8x10 mm and 10x10 mm (Width x Height) as shown in Figure 4.9. We only considered the Von Mises stresses as a comparable parameter because other parameters can't be compared because the dimensions of the plate are changing. We will be demonstrating numerical analysis of two shapes only due to space constraints in Figure 4.9, Von Mises stresses of all 6 shapes are compared in Graph 4.5.

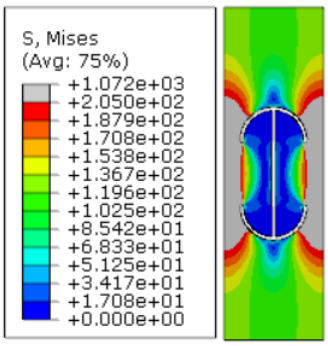

3x10 mm plate with Double T shape

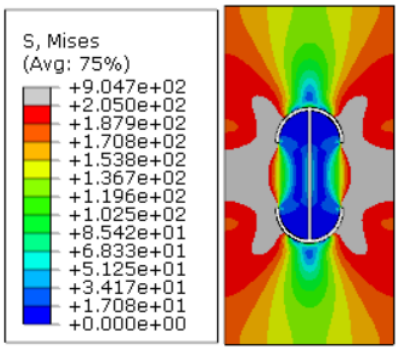

5x10 mm plate with Double T shape

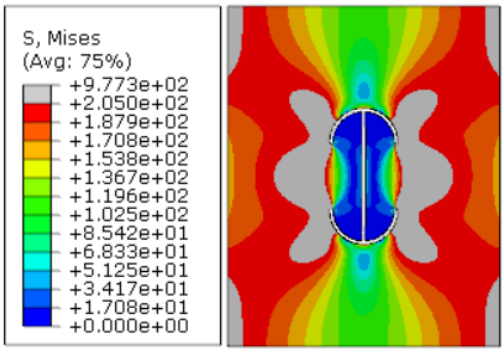

8x10 mm plate with Double T shape

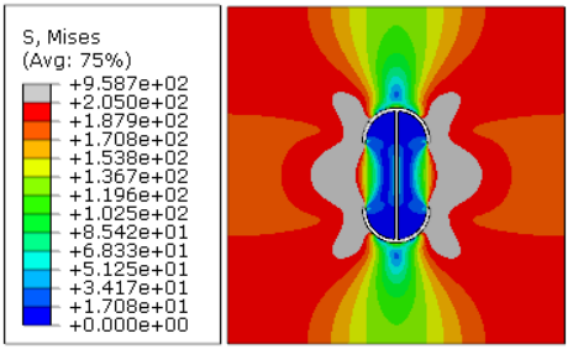

10x10 mm plate with Double T shape

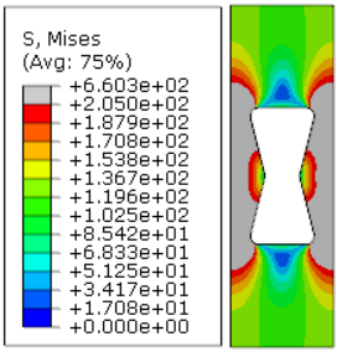

3x10 mm plate with Hourglass shape

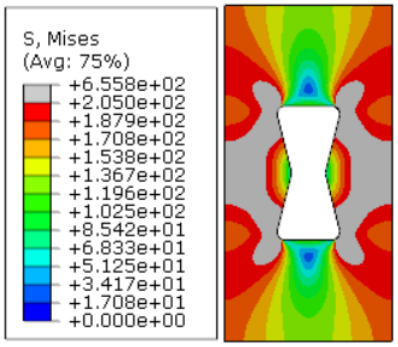

5x10 mm plate with Hourglass shape

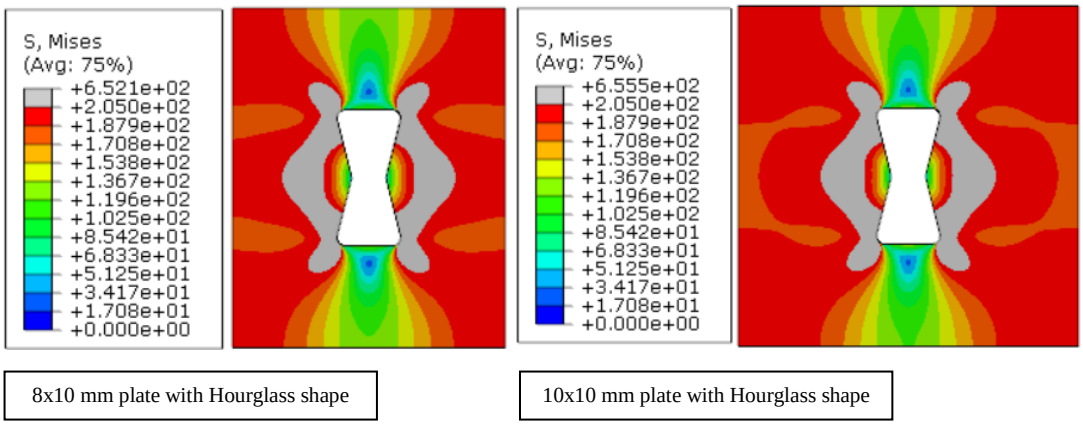

Figure 4.9 Numerical Analysis of shapes with Influence of Width

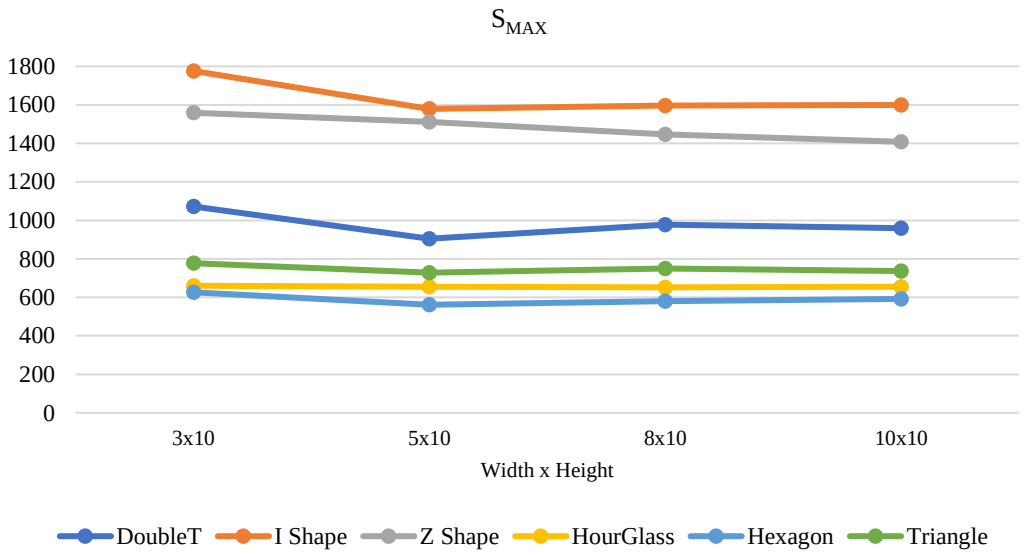

Graph 4.5 Plots of maximum Von Mises Stresses based on the Influence of Width

Based on numerical analysis on the influence of width we have obtained the maximum Von Mises stresses which have been plotted in Graph 4.5. We can observe that the thick shapes which are Hourglass, Hexagon and Triangle induce fewer stresses when compared to thin shapes which are Double T, I shape and Z shape based on width analysis. The influence of width reduces with increase in width based on the plots obtained in Graph 4.5, we can clearly observe that the stresses plots become straight when the width is increased from 3mm to 10mm. Also, there is a reduction of stresses with an increase in width which infers that the closer the patterns they can induce more stresses locally than they are far apart. This analysis was considered based on medium sized shapes with only 1 pattern if we consider more patterns the stresses might change depending on the shape.

4.2.6. Influence of Porosity using Patterns.

All the design conditions above were performed with constant porosity value as they influence the measuring parameters considerably. But we are going to analyze with an increase in porosity we can observe positive aspects to design our metallic perforated sheets to have better stress filed distribution. To conduct this analysis we have considered two shapes (Double T, Hourglass) with six range of porosity values three for thick structured shape and three for a thin structured shape. So, we have designed with 6%, 23.6% and 47.2% for Hourglass shape (thick structured shaped), then 1%, 4% and 8% for Double T shape (thin structured shape) as shown in Figure 4.10.

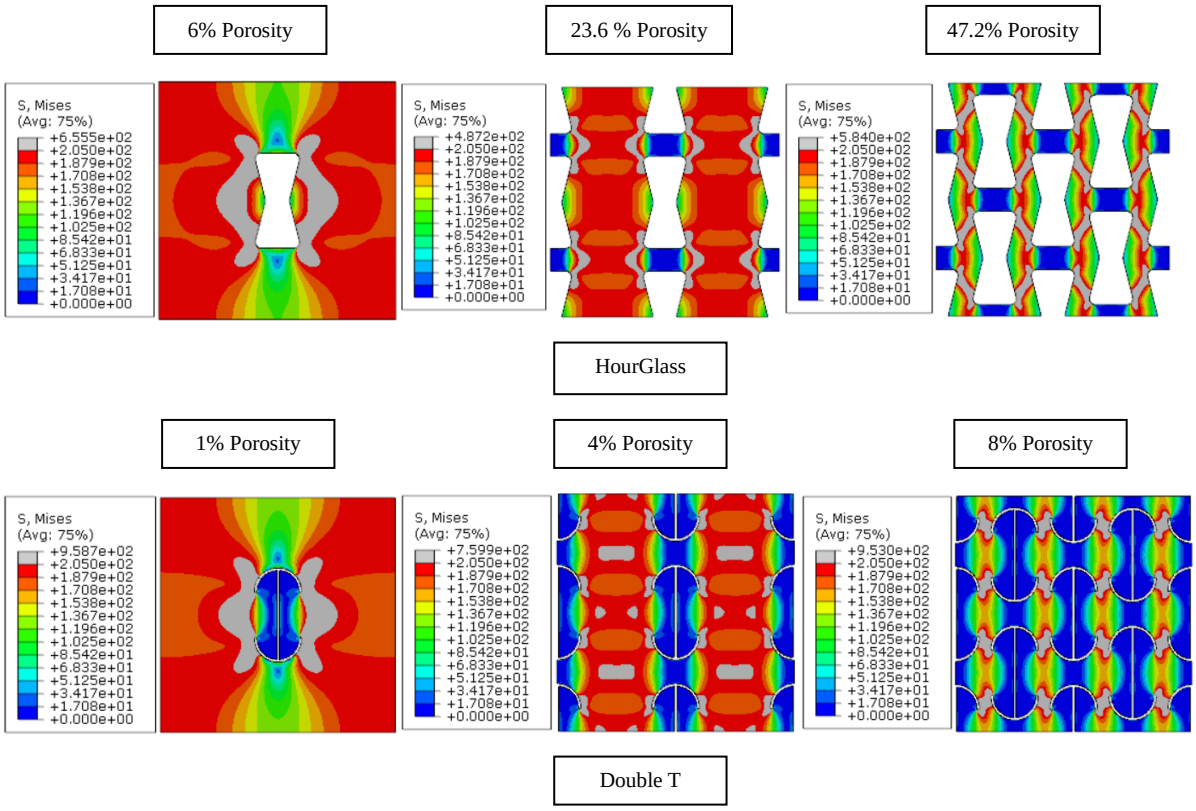

Figure 4.10 Numerical Analysis of shapes with Influence of Porosity

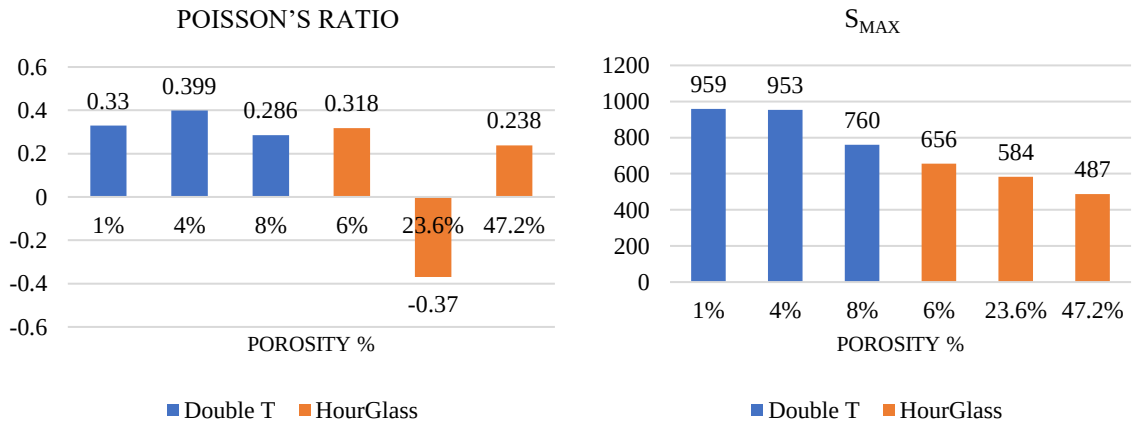

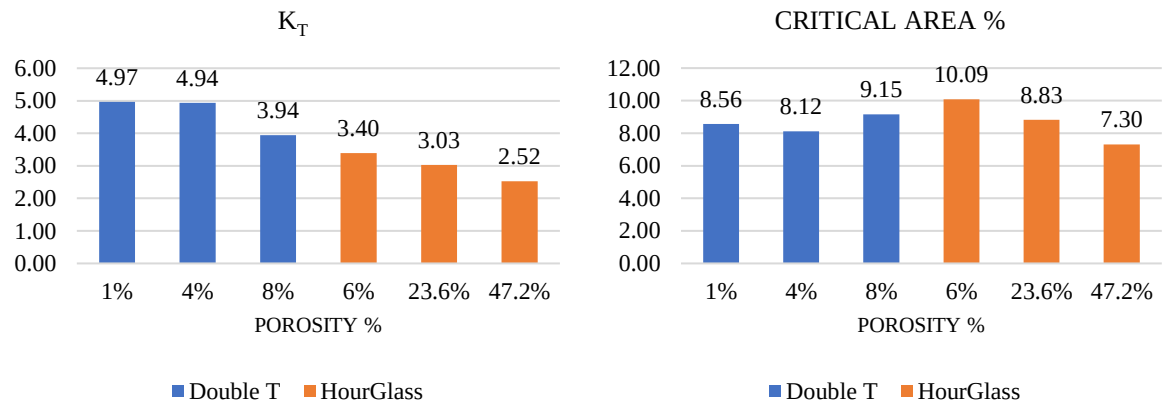

Graph 4.6 Bar plots of measured parameters with the Influence of Porosity

Based on the numerical analysis of the two shapes we have obtained the bar plots of the measuring parameters in Graph 4.6. If we observe the Von Mises stresses (S_{MAX}) and Stress concentration factor (K_T) with an increase in porosity the stresses decreases in both Double T and Hourglass shapes. It may be because the stresses are shared by a number of patterns which increases in numbers based on porosity incrementation. But in case of Critical Area for thick structured shape (Hourglass), it is clearly evident that it decreases with the increase of porosity but that's not the case with the thin structured shape (Double T) it is fluctuating which depends on the behavior of patterns. Hence, Hourglass shape has obtained the least stresses at 47.2% porosity and Double T shape has obtained least stresses at 8% porosity based on Graph 4.6.

If we observe Poisson's Ratio value for both the shapes it behaves in an unpredictable manner which seems to be dependent on the profiles of the shapes. We have obtained negative Poisson,s ratio of -0.37 for the Hourglass shape at 23.6% porosity value and for Double T shape, we have obtained 0.286 Poisson's Ratio value at 8% porosity which is its least value. Hence Porosity fluctuates the Poisson's Ratio value so we should fix the porosity value when comparing the Poisson's Ratio values.

4.3. TOPOLOGY OPTIMIZATION

Topology optimization is a mathematical method that optimizes material layout within a given design space, for a given set of loads, boundary conditions and constraints with the goal of maximizing the performance of the system. After performing numerical analysis on various design conditions discussed above we have understood the pattern behavior on the measuring parameters. But, using Topology optimization we are going to analyze the capability of our shapes to reach its maximum performance with slight changes keeping the same load conditions and meshing parameters.

Optimization constraints

Using Abaqus Topology optimization module we can perform the optimization on our models with specific design constraints to obtain the preferred Topology. So keeping stresses as the variable to be lowest and volume being the control parameter we performed the optimization process for all our shapes. We have controlled the optimization with a volume reduction of 40%, 30%, 25%, and 20% which gave us four solutions and we have finalized 25% volume reduction will be the most preferred solution. The Topology optimized results are as follows:

Original Shape | Topology Optimization | Modified Shape

a) Double T

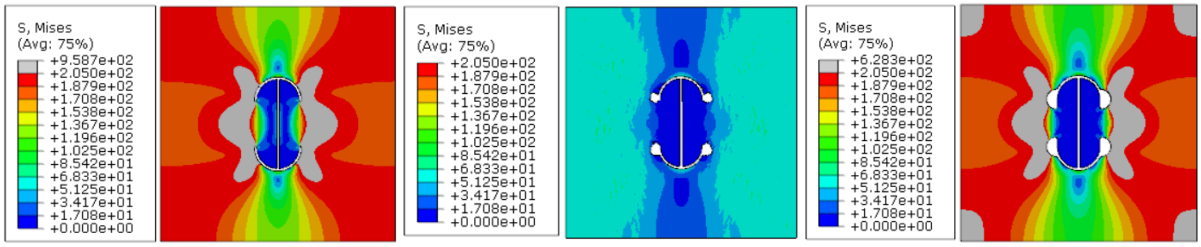

Figure 4.11 Topology Optimization of Double T Shape

We can observe there is a decrease of Maximum Von Mises stresses from 958.7 MPa to 628.3 MPa in a modified shape. But there is an increase in Critical Area than the original shape with a very slight change in Poisson's Ratio from 0.33 to 0.326.

b) Z Shape

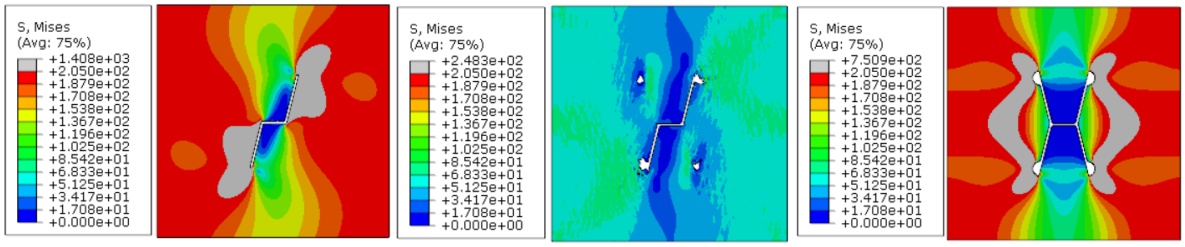

Figure 4.12 Topology Optimization of Z Shape

Based on the solution obtained by Topology optimization for Z shape we have a drastic profile change to H shape which has reduced Maximum Von Mises stresses from 1408 MPa to 750.9 MPa. Also, the Poisson's Ratio value has dropped from 0.309 to 0.284 with increased Critical Area.

c) Triangle

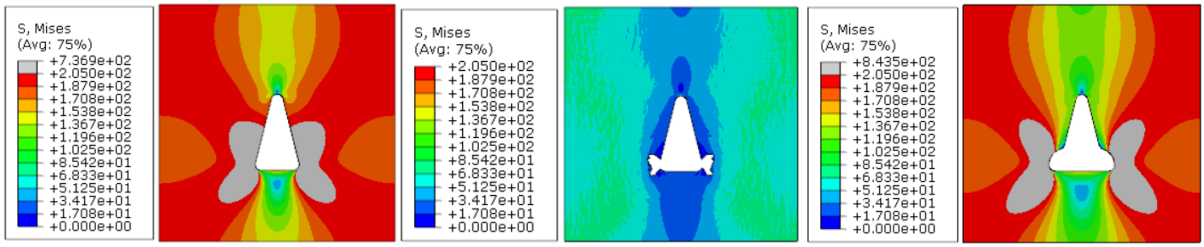

Figure 4.13 Topology Optimization of Triangle Shape

The solution provided by the Topology analysis for the triangle shape was not reliable as it has increased the Maximum Von Mises stresses from 736.9 MPa to 843.5 MPa with a slight decrease of Poisson's Ratio and increase Critical Area.

d) Hexagon

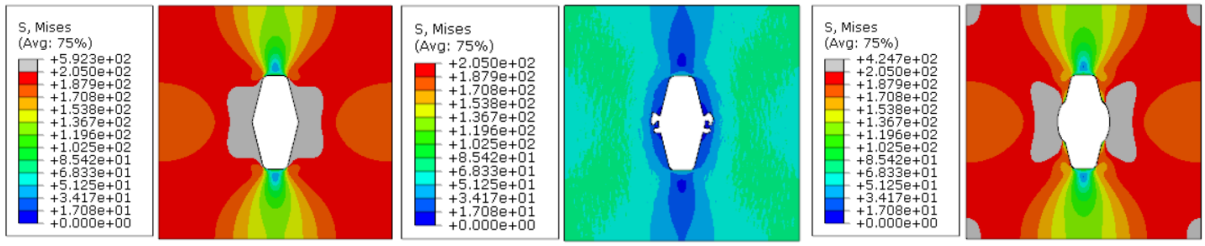

Figure 4.14 Topology Optimization of Hexagon Shape

Hexagon shape Topology optimization results have reduced Von Mises stresses from 592.3 MPa to 424.7 MPa without a change in Poisson's Ratio. There is a slight increase in Critical Area at the edges on the plate based on Modified shape numerical analysis.

e) Hourglass

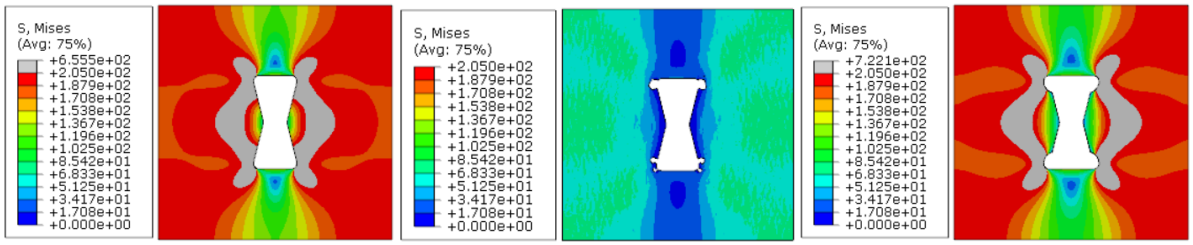

Figure 4.15 Topology Optimization of Hourglass Shape

The Hourglass shape Topology Optimization has increased the Von Mises stresses from 655 Mpa to 722 Mpa with a slight change in Poisson's Ratio and increased Critical Area.

So based on the solutions obtained by Topology optimization above we can observe that the software has removed material were the stresses were maximum. Through which we reshaped it using curvy profiles to distribute those localized stresses which have given such complex

shapes. Except for the Triangle and Hourglass, shape gave the maximum Von Mises stresses were reduced considerably with very less effect on Poisson's Ratio and Critical Area. But the best solution which can be retained is the modification of Z shape to H shape which has a huge reduction of stress values and its distribution. The main disadvantage of these modifies shape would be the machining process with such complex profiles and tighter tolerances. Hence, depending on the application demand only then these Modified shapes can be accepted.

5. CONCLUSION

The aim of this study was analyzing 2D perforated patterns using Periodic Boundary Conditions to have better stress field and enhance its mechanical properties for its usage in various applications. Before designing new shapes and analyzing them we understood the measuring parameters (discussed in chapter 4) used to evaluate and validate them by two case studies discussed in section 3.1.1 and 3.1.2. The first case study (section 3.1.1) gave us insight regarding the auxetic behavior of four different shapes and the computation of Poisson's Ratio through the horizontal and vertical displacements. The second case study (section 3.1.2) which was based on porous structures stress study using Periodic Boundary Conditions introduced us to the measuring parameters related to perforated patterns and the stress distribution of a metallic perforated plate under the influence of static tensile load.

Consequently, we selected pore shapes based on references [2, 5-8] and tested them in six design conditions. Beginning with the Influence of size (section 4.2.1) it was observed that the large-sized shapes were giving the most negative values of Poisson's Ratio when compared to the small and medium-sized shapes. Also, most of the shapes exhibited lower Von Mises stresses in large size when compared to lower sizes except the Triangle shape whose stresses incremented with the increase in size because of its edges which were becoming sharper with the influence of size. Then moving on to the influence of arrangement (section 4.2.2) we understood the connection between the direction of loading and arrangement of patterns. Our load being in the vertical direction we got lower Poisson's Ratio values described in Graph 4.2 in horizontal and alternate configurations compared to the vertical configuration of patterns. But, Von Mises stresses and Critical Area was depending on the shape in which Double T, Hexagon, and Hourglass gave us the best results in all the three configurations. Further, we studied the influence of profile (section 4.2.3) were the sharper edges of Triangle, Hexagon, Hourglass and Z shape was removed with large fillets which reduced their stresses considerable but with the sacrifice of Poisson's Ratio based on Graph 4.3. Which means that fillets or circular profiles reduces the auxetic effect in the perforated metal sheets and increases the Critical Area. Rotating the patterns (section 4.2.4) in four different angles made us aware regarding the stress distribution of near edges changes with the angle of patterns. The Von Mises stresses were higher in 45^0 and 135^0 angles due to the flow of stresses from edge to edge between the patterns in angular stress distribution when compared with 90^0 and 180^0 contour plots. Analyzing the distance between the patterns (section 4.2.5) by reducing the width of the plate thicker shapes (Hourglass, Hexagon, and Triangle) exhibited lower Von Mises stresses

when compared to thinner shapes (Double T, Z Shape and I Shape). The influence of the width on the stresses reduces with the increase in width which infers that the closer the patterns they can induce more stresses locally than they are far apart. The final design condition was based on the Influence of Porosity (section 4.2.6) which highly changes the measuring parameters. So, with an increase in porosity, we observed a decrease in Von Mises stresses for Double T and Hourglass shapes but the Poisson's Ratio was clearly dependent on the pore shape behavior because of that it was fluctuating.

The final possibility to optimize the shapes we choose was to apply topology optimization which was based on stress reduction by changing the volume of the plate. The solutions obtained was dependent on the shapes in which the Triangle and Hourglass shape gave the maximum Von Mises stresses were reduced considerably with very less effect on Poisson's Ratio and Critical Area. But the best solution which can be retained is the modification of Z shape to H shape which has a huge reduction of stress values and its distribution. Moreover, solutions obtained by topology optimization will increase the complexity of machining the patterns which will hamper the manufacturing cost.

Hence, based on the results of numerical analysis of our shapes on all design conditions (section 4.2) we discussed the most satisfying results with some trade-offs we have achieved Double T pattern in case of thin structures shapes and Hourglass pattern in case of the thick structured pattern. Both these patterns will improve the stress field distribution of perforated metallic sheets with low-stress values with enhanced auxetic behavior for the applications they are demanded.

6. REFERENCES

[1] Farhad Javid, Jia liu, Ahmad Rafsanjani, Megan Schaenzer, Minh Quan Pham, David Backman, Scott Yandt, Matthew C.Innes, Christopher Booth-morrison, Miklos gerendas, Thomas Scarinci, Ali Shanian, Katia Bertoldi - *On the design of porous structures with enhanced fatigue life* – 16 (2017) 13-17

[2] L. Francesconi, M. Taylor, K. Bertoldi, A. Baldi - *Static and Modal Analysis of Low Porosity Thin Metallic Auxetic Structures Using Speckle Interferometry and Digital Image Correlation* - 58 (2018) 283–300

[3] Michael Taylor, Luca Francesconi, Miklos Gerendas, Ali Shanian, Carl Carson and Katia Bertoldi - *Low porosity metallic periodic structures with negative Poisson's Ratio*, Adv.mater.26 (15) (2014) 2365-2370

[4] Weidong Wu, Joseph Owino, Ahmed Al-Ostaz, Liguang Cai - *Applying periodic boundary conditions in Finite Element Analysis* – 2014 SIMULIA Community Conference

[5] Luke Mizzi, Keith M. Azzopardi, Daphne Attard1, Joseph N. Grima1and Ruben Gatt* - *Auxetic metamaterials exhibiting giant negative Poisson's Ratios* Phys. Status Solidi RRL 9, 7, (2015) 425-430

[6] Sicong Shana, Sung H. Kanga,b, Zhenhao Zhaoa, Lichen Fang, Katia Bertoldi - *Design of planar isotropic negative Poisson's Ratio structures* - 4 (2015) 96–102

[7] Mohammad Jafari, ElaheArdalani – Stress concentration in finite metallic plates with regular holes – 106 (2016) 220–230

[8] Hubert Jopek and Tomasz Stręk - *Thermoauxetic Behavior of Composite Structures* – 24 (2018) 60-965

[9] McNICHOLS® - *How perforated Metal made? (www.mcnichols.com)* – (2019)

[10] Joseph N. Grima, Luke Mizzi, Keith A. Azzopardi, and Ruben Gatt - *Auxetic perforated mechanical metamaterials with randomly oriented cuts* – adv.mater 28 (2) (2015)

[11] Andreas Gruner, Joerg Schille, Udo Loeschner - *Experimental study on micro hole drilling using ultrashort pulse laser radiation* – physics procedia 83 (2016) 157 - 166

[12] David Gillen and David Moore - *TinyTriumphs: Laser drilling Micron-sized holes* – 2012 Blue care technology Ltd, Dundalk, Co Louth, Ireland

[13] R.Patwa, H.Herfurth, C.Bratt - *Laser drilling of micro-hole arrays in Tantalum – Journal of laser applications* - 27 (S2) (2015)

[14] Xiangwen Zhang and Deqing Yang - *Mechanical Properties of Auxetic Cellular Material Consisting of Re-Entrant Hexagonal Honeycombs* - Published: 7 November 2016

7. APPENDIX A

PYTHON CODES

A.1. Code to insert dimensions, create a reference point and apply displacement control on the plate.

```
#Execution conmmand for 'AbaqusScriptFunc.py' file
Mdb()
execfile('AbaqusScriptFunc.py')
##############################################################################
#CREATE PERIODIC BOUNDARY CONDITIONS
##############################################################################
mdb.models['Model-1'].rootAssembly.Set(edges=(
    mdb.models['Model-1'].rootAssembly.instances['Instance-1'].edges,),
name='PerBound')
#Plate dimensions are 10x10 mm , so our cordinates are (0,10),(10,0)
(CoorFixNode,NameRef1, NameRef2)=PeriodicBound2D(mdb,'Model-
1','PerBound',[(0.0,10),(10,0.0)],)
##############################################################################
#CREATE STEP AND APPLY BC
##############################################################################
mdb.models['Model-1'].StaticStep(name='Step-1', nlgeom=ON, previous='Initial')
#Apply boundary conditions on reference nodes
DefMat=[(UNSET,0.01),(UNSET,UNSET)]
mdb.models['Model-1'].DisplacementBC(amplitude=UNSET, createStepName='Step-1',
    distributionType=UNIFORM, fieldName='', fixed=OFF, localCsys=None, name=
    'BC-REF-1', region=Region(referencePoints=(
    mdb.models['Model-1'].rootAssembly.instances[NameRef1].referencePoints[1],
    )), u1=DefMat[0][0], u2=DefMat[0][1], ur3=UNSET)
mdb.models['Model-1'].DisplacementBC(amplitude=UNSET, createStepName='Step-1',
    distributionType=UNIFORM, fieldName='', fixed=OFF, localCsys=None, name=
    'BC-REF-2', region=Region(referencePoints=(
    mdb.models['Model-1'].rootAssembly.instances[NameRef2].referencePoints[1],
    )), u1=DefMat[1][0], u2=DefMat[1][1], ur3=UNSET)
mdb.models['Model-1'].DisplacementBC(amplitude=UNSET, createStepName='Step-1',
    distributionType=UNIFORM, fieldName='', fixed=OFF, localCsys=None, name=
    'BC-FIXNODE', region=Region(
    nodes=mdb.models['Model-1'].rootAssembly.instances['Instance-
1'].nodes.getByBoundingSphere(center=CoorFixNode, radius=0.001)), u1=0.0, u2=0.0,
ur3=0.0)

##############################################################################
#JOB AND RUN
##############################################################################
mdb.Job(atTime=None, contactPrint=OFF, description='', echoPrint=OFF,
    explicitPrecision=SINGLE, getMemoryFromAnalysis=True, historyPrint=OFF,
    memory=90, memoryUnits=PERCENTAGE, model='Model-1', modelPrint=OFF,
    multiprocessingMode=DEFAULT, name='Job-1', nodalOutputPrecision=SINGLE,
    numCpus=1, queue=None, scratch='', type=ANALYSIS, userSubroutine='',
    waitHours=0, waitMinutes=0)
mdb.jobs['Job-1'].submit(consistencyChecking=OFF)
```

A.2. Applying Periodic Boundary Conditions to the model

```
#FUNCTION TO APPLY PERIODIC BOUNDARY CONDITIONS IN 2D
#mdb: model database
#NameModel:   A string with the name of your model
#NameSet:     A string with the name of your set (for a faster script, this set
#             should only contain those nodes that will have periodic boundary
conditions applied to them)
#LatticeVec: An array with the lattice vectors, for example [(1.0, 0.0), (1.0,
1.0)] for a square lattice
def PeriodicBound2D(mdb,NameModel,NameSet,LatticeVec):
```

```
    from part import TWO_D_PLANAR, DEFORMABLE_BODY
    #Create reference parts and assemble
    NameRef1='RefPoint-0'; NameRef2='RefPoint-1'
    mdb.models[NameModel].Part(dimensionality=TWO_D_PLANAR, name=NameRef1, type=
        DEFORMABLE_BODY)
    mdb.models[NameModel].parts[NameRef1].ReferencePoint(point=(0.0, 0.0, 0.0))
    mdb.models[NameModel].Part(dimensionality=TWO_D_PLANAR, name=NameRef2, type=
        DEFORMABLE_BODY)
    mdb.models[NameModel].parts[NameRef2].ReferencePoint(point=(0.0, 0.0, 0.0))
    mdb.models[NameModel].rootAssembly.Instance(dependent=ON, name=NameRef1,
        part=mdb.models[NameModel].parts[NameRef1])
    mdb.models[NameModel].rootAssembly.Instance(dependent=ON, name=NameRef2,
        part=mdb.models[NameModel].parts[NameRef2])
    #Create set of reference points
    mdb.models[NameModel].rootAssembly.Set(name=NameRef1, referencePoints=(

mdb.models[NameModel].rootAssembly.instances[NameRef1].referencePoints[1],))
    mdb.models[NameModel].rootAssembly.Set(name=NameRef2, referencePoints=(

mdb.models[NameModel].rootAssembly.instances[NameRef2].referencePoints[1],))
    #Get all nodes
    nodesAll=mdb.models[NameModel].rootAssembly.sets[NameSet].nodes
    nodesAllCoor=[]
    for nod in mdb.models[NameModel].rootAssembly.sets[NameSet].nodes:
        nodesAllCoor.append(nod.coordinates)
    repConst=0
    #Find periodically located nodes and apply equation constraints
    ranNodes=range(0,len(nodesAll))     #Index array of nodes not used in equations
constraint
    for repnod1 in range(0,len(nodesAll)):
        stop=False               #Stop will become true when equation constraint is
made between nodes
        Coor1=nodesAllCoor[repnod1]            #Coordinates of Node 1
        for repnod2 in ranNodes: #Loop over all available nodes
            Coor2=nodesAllCoor[repnod2] #Coordinates of Node 2
            dx=Coor2[0]-Coor1[0]; dy=Coor2[1]-Coor1[1]      #X and Y Distance
between nodes
            for comb in range(0,len(LatticeVec)):    #Check if nodes are located
exactly the vector lattice apart
                if int(round(1000.0*(LatticeVec[comb][0]-dx)))==0:
                    if int(round(1000.0*(LatticeVec[comb][1]-dy)))==0:
                        #Correct combination found
                        #Create sets for use in equations constraints
                        mdb.models[NameModel].rootAssembly.Set(name='Node-1-
'+str(repConst), nodes=

mdb.models[NameModel].rootAssembly.sets[NameSet].nodes[repnod1:repnod1+1])
                        mdb.models[NameModel].rootAssembly.Set(name='Node-2-
'+str(repConst), nodes=

mdb.models[NameModel].rootAssembly.sets[NameSet].nodes[repnod2:repnod2+1])
                        #Create equations constraints for each dof
                        for Dim1 in [1,2]:

mdb.models[NameModel].Equation(name='PerConst'+str(Dim1)+'-'+str(repConst),
                                terms=((1.0,'Node-1-'+str(repConst), Dim1),(-1.0,
'Node-2-'+str(repConst), Dim1) ,
                                       (1.0, 'RefPoint-'+str(comb), Dim1)))
                        repConst=repConst+1    #Increase integer for naming
equation constraint
                        ranNodes.remove(repnod1)#Remove used node from available
list
                        stop=True       #Don't look further, go to following node.
                        break
            if stop:
                break
    #Return coordinates of free node so that it can be fixed
    return (nodesAll[ranNodes[0]].coordinates, NameRef1, NameRef2)
```